Fall 1991

# Simulation and modeling of kinetics of silicon oxidation in the thin oxide regime

Tirthankar Dutta
*New Jersey Institute of Technology*

# Copyright Warning & Restrictions

The copyright law of the United States (Title 17, United States Code) governs the making of photocopies or other reproductions of copyrighted material.

Under certain conditions specified in the law, libraries and archives are authorized to furnish a photocopy or other reproduction. One of these specified conditions is that the photocopy or reproduction is not to be "used for any purpose other than private study, scholarship, or research." If a, user makes a request for, or later uses, a photocopy or reproduction for purposes in excess of "fair use" that user may be liable for copyright infringement,

This institution reserves the right to refuse to accept a copying order if, in its judgment, fulfillment of the order would involve violation of copyright law.

Please Note: The author retains the copyright while the New Jersey Institute of Technology reserves the right to distribute this thesis or dissertation

Printing note: If you do not wish to print this page, then select "Pages from: first page # to: last page #" on the print dialog screen

# ABSTRACT

Title of Thesis: Simulation and Modeling of Kinetics of Silicon Oxidation in the thin oxide regime

Tirthankar Dutta, Master of Science, Electrical Engineering Department, 1991

Thesis directed by: Dr. N.M.Ravindra, Associate Professor

Thermal oxidation of Silicon in dry $O_2$, in the thin regime($< 500\mathring{A}$) is of vital importance to VLSI device engineers, because thin layers of $SiO_2$ are exclusively used as gate dielectric for high performance of MOS devices. There exist a number of models to explain the kinetics of oxidation in this thin regime. However there is considerable variance among them and the reported rate constants, which are supposed to describe the oxidation process. Rather than arriving at an alternative model, the present study aims at an extensive study and simulation of existing models of oxidation in dry oxygen, in the thin regime, with a recent set of experimental data and arrive at the best possible model and provide accurate rate constants for oxidation in dry oxygen. These experimental data have been obtained, earlier, using high-resolution transmission electron microscopy (HRTEM) and ellipsometry techniques to measure thicknesses of silicon oxide, grown at $800°C$ in dry oxygen, in the thickness range of 2-20 nm.

# Simulation and Modeling of Kinetics of Silicon Oxidation in the thin oxide regime

by

Tirthankar Dutta

Thesis submitted to the Faculty of the Graduate School of
the New Jersey Institute of Technology
in partial fulfillment of the requirements for the degree of
Master of Science in Electrical Engineering.
Dec 1991.

To My Parents

and

My Wife

# ACKNOWLEDGEMENT

First and foremost, I would like to express my gratitude and appreciation to my advisor Dr. N. M. Ravindra, for his invaluable guidance in this research and the financial support. I gratefully acknowledge Dr. K. Sohn and Dr. D. Misra, for consenting to be on my thesis committee and reviewing this thesis.

I am greatly indebted to my parents and my wife, for their constant encouragement and moral support, which has enabled me to achieve this goal.

# VITA

Name: TIRTHANKAR DUTTA

Address: 664 Elm Street, Kearny, NJ 07032

Degree and date to be conferred: MSEE, 1991

| Collegiate institutions attended | Dates | Degree | Date of Degree |
|---|---|---|---|
| Jadavpur University, Calcutta, India | 1982-1986 | BSEE | Dec. 1986 |
| New Jersey Institute of Technology, NJ | 1990-1991 | MSEE | Dec. 1991 |

Major: Electrical Engineering

# APPROVAL SHEET

Title of Thesis: Simulation and Modeling of Kinetics of Silicon Oxidation in the thin oxide regime

Name of Candidate: TIRTHANKAR DUTTA
Master of Science in Electrical Engineering, 1991

Thesis and Abstract Approved:

Dr. N. M. Ravindra — Date
Associate Professor
Physics Department

Dr. K. Sohn — Date
Professor
EE Department

Dr. D. Misra — Date
Assistant Professor
EE Department

# Contents

# List of Figures

# List of Tables

# Chapter 1

# Introduction

## 1.1 An Overview

The oxidation of Silicon is necessary during the entire process of fabricating modern integrated circuits. The production of high-quality ICs requires not only an understanding of the basic oxidation mechanism, but the ability to form in a controlled and repeatable manner a high quality oxide. Thus, the growth of Silicon dioxide by thermal oxidation has been a critical step in semiconductor processing since the very inception of the microelectronics industry. The ability to reliably obtain a uniform dielectric layer of virtually any thickness that can be patterned as necessary is crucial to the production of every modern Silicon based device.

With devices approaching submicrometer dimensions, production and characterization of highly reliable ultrathin Silicon dioxide films are assuming major im-

portance in very large-scale integration (VLSI) technology. The thermal oxidation of Silicon in the thin regime ($< 500\mathring{A}$) is of vital importance to VLSI device designers because thin layers of $SiO_2$ are exclusively used as the gate oxides, requiring a low thermal budget, compatible with the rest of the processing steps involved in Silicon technology[1]. The thin gate dielectric ensures high performance MOS devices. This regime has received much attention, but it still remains unexplained with respect to the oxidation mechanism.

### 1.1.1 Importance of Thin and Native Oxides

As already mentioned, recent developments have a continuing impetus to reduce the dimensions of semiconductor devices which is motivated both by the attraction of further miniaturization in high-technology applications and by the economic incentive of producing a large number of more powerful circuits with the same amount of raw material. The philosophy underneath the very-large-scale and ultra-large-scale integration (VLSI and ULSI) lies in assimilation of many components on a single solid-state chip, and thus require that each individual device be made as small as possible. Thus, the dielectric layer has to be scaled down accordingly. Current gate oxides for MOS technology are approaching thicknesses of 10 nm or less. Thinner oxides are also necessary for some memory applications including erasable and electrically erasable read- only memories (EPROMs and EEPROMs, respectively). Reliable production of thin $SiO_2$ is therefore central to continued progress in silicon device fabrication. The uniformity of the thin film and interface structures is critical in device operations; deviations can cause premature oxide breakdown, reductions in efficiency, and impairment of the solid-state circuits' function.

Native oxide layers are formed when Silicon wafers are exposed to air at room temperature. They provide the starting point for Silicon oxidation, and an un-

derstanding of them is necessary to unravel the details of the initial oxide growth kinetics and interface structure. Further, the intentional or inadvertent presence of a native oxide layer can affect subsequent processing steps. For instance, the gain available through polysilicon emitter transistor structures may be enhanced by the addition of a thin interfacial oxide layer [2,3], although speed and transconductance are ordinarily sacrificed [4]. Metal deposition rates can be substantially affected by the thickness of an existing native oxide layer [5].

### 1.1.2 Thin oxide growth kinetics

The oxidation of single-crystal silicon was first described by Deal and Grove in 1965 [6]. They developed a linear-parabolic governing equation that successfully fit the existing data, and is given by,

$$\frac{X_o^{\,2}}{B} + \frac{X_o}{B/A} = t + \tau \tag{1.1}$$

where, $X_o$ is oxide thickness, t is oxidation time, B and B/A are process-dependant rate constants, and $\tau$ is a correction factor that adjusts for the native oxide thickness or initial growth, that is not accounted for by the model. This model is based on some arguable physical assumptions e.g steady state is possible in solid state diffusion, and linear and diffusion specific rate constants can be rate limiting at the same time. More important is the fact that this model does not provide even an approximate fit to oxidation data below about 350$\mathring{A}$, giving rise to a so-called "anomalous oxidation region". Deal and Grove found that there was an initial accelerated growth rate when oxidation was performed in a dry $O_2$ ambient. The physical reasons for this were not clear and therefore they simply used the parameter $\tau$ to correct for this effect without attempting to specify a mathematical expression describing the initial regime.

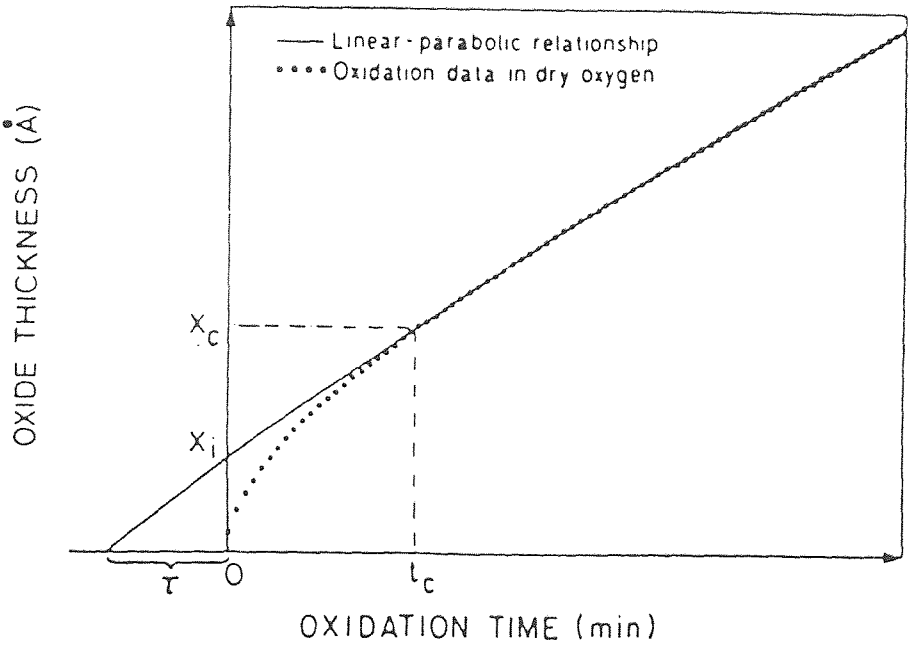


Figure 1.1: The fit of the linear-parabolic relationship to oxidation data in dry oxygen

As Silicon technology has progressed to smaller and smaller dimensions (and accordingly thinner oxides), this anomalously fast growth regime has assumed considerable practical importance. The primary initial oxidation data currently available are from ellipsometry as well as from High Resolution Transmission Electron Microscopy(HRTEM).

A number of different forms and mechanisms have been suggested for the initial thin oxide growth relationship. The proposals in the literature have included schemes based on enhanced oxidant diffusion [7], reduced oxidant diffusivity in the oxide [8], fixed charge effects on the interface reaction rate [9]. Linear, parabolic and several other relationships for the initial growth have been proposed. Rather than surveying the various possibilities here, a review of current models are included in the subsequent chapters.

## 1.2 Objectives of the current work

This study focuses on the growth kinetics of $SiO_2$ layers in the thin regime ($< 500\text{Å}$) in order to achieve a better understanding of the oxidation process, particularly in the thin oxide region. The present thesis describes the experimental procedures used to study the oxidation kinetics and the data analysis techniques used to fit the best model to a set of experimental data and subsequently arrive at new constants for further interpretation. With the help of the newly obtained constants, a computer program has been coded to simulate the proposed model and the output was compared with the actual experimental data.

The intention in this research is also to remark on the implications of the current oxide thickness measurements after measuring the absolute thicknesses of the oxide layers by HRTEM and compare these measurements to that obtained by ellipsometry. The study also aims at finding the reasons for the larger discrepancies in the reported rate constants.

## 1.3 Organization of the Thesis

Although a variety of models were discussed, the main part of the research was to throw light on the initial regime, with the help of the experimental data available from both ellipsometry as well as HREM measurements. The theory behind oxidation and the pioneering model set by Deal and Grove is described in Chapter 2. Chapter 3 discusses the different oxidation techniques, but the specific procedures for particular experiments are given in the subsequent chapters. Chapter 4 reviews models for the anomalously fast initial growth of oxide in dry oxygen with special light on the experimental procedures followed by different researchers. Chapter 5 contains the experimental techniques involved in this research along with the data

analysis procedures followed. Chapter 6 details the results, the analysis of data and their fit to different models and the rate constants. Chapter 7 narrates the Conclusion of the analysis and scope of further development.

A program with the calculated constants, obtained from the fit written in *C*, to simulate the proposed model. The source code along with the output is presented in the Appendix.

# Chapter 2

# Silicon Oxidation

## 2.1 Introduction

Semiconductors can be oxidized by various methods. These include thermal oxidation in both dry and wet environment, electrochemical anodization and plasma reaction. Among these methods thermal oxidation is by far the most important for Silicon devices. It is the key process in modern Silicon integrated circuit technology [10]. Oxide layers in Silicon IC technology provide the following :

(1) Surface passivation for a silicon device.

(2) Serve as a diffusion mask.

(3) Serve to isolate one device from another.

(4) Serve to insulate the gate electrode from the Silicon in field effect devices.

(5) Serve to isolate multiple levels of device interconnection in an IC.

For gate oxides in field effect devices such as the MOSFET and the CCD, the oxide-semiconductor interface again must have a minimum, stable density of oxide fixed charge and interface traps, but now stability is especially important[11]. The oxide that meets these requirements best is thermally grown oxide. For these reasons, thermal growth is the key oxidation process in integrated circuit technology.

## 2.2 Oxide Formation

The basic oxidation process is the sharing of valence electrons between Silicon and Oxygen to form four Silicon-oxygen bonds. Each bond is largely covalent with a small ionic component at room temperature.

It is shown (Marker experiments)[11] that an oxidizing species and not silicon moves across the oxide layer and that the oxidation reaction occurs at the silicon-oxide interface. During oxidation the top surface of the $SiO_2$ film will not be coplanar with the original silicon surface because a volume expansion occurs during oxidation. This expansion occurs because the density of $SiO_2$ (2.21 g/$cm^3$) is slightly less than the density of Silicon (2.33 g/$cm^3$). Growth of an oxide of thickness $X_o$, will consume a layer of Silicon about $0.45X_o$ thick, as can be calculated from the density and molecular weight of Silicon and $SiO_2$ [10]. Fig 2.1 gives a rough idea of the mentioned phenomonea.

For oxidation in pure oxygen, which produces "dry" oxides, the stoichiometric chemical reaction producing the oxide film is

$$Si(solid) + O_2 \rightleftharpoons Si0_2(solid) \tag{2.1}$$

The stoichiometric chemical reaction for producing the oxide film in water vapour "wet oxides" is

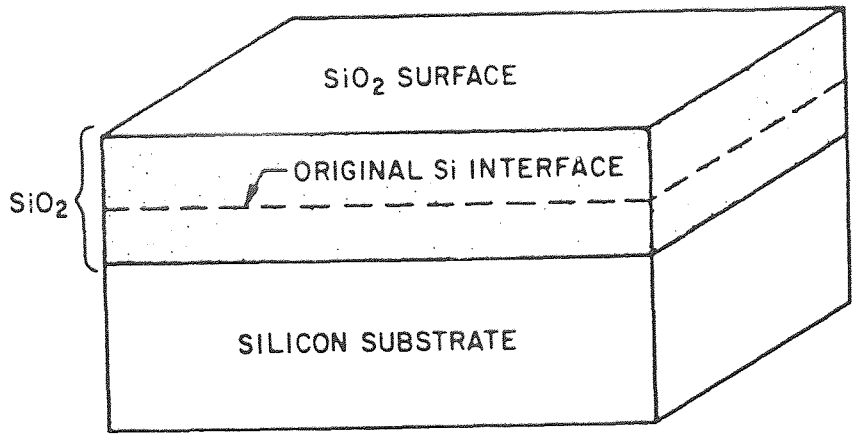


Figure 2.1: Growth of Silicon dioxide by thermal oxidation

$$Si(solid) + 2H_2O = SiO_2 + 2H_2 \tag{2.2}$$

Reaction (2.1) describes the overall reaction between oxygen and Silicon, and reaction (2.2) describes that between water vapour and Silicon.

The basic structural unit of thermally grown Silicon dioxide is a Silicon ion surrounded tetrahedrally by four oxygen ions as illustrated in Fig 2.2(a). The Silicon-to-oxygen internuclear distance is 1.6Å and the oxygen -to -oxygen internuclear distance is 2.27Å. These tetrahedra are joined together at their corners by oxygen bridges in a variety of ways to form the various phases or structures of Silicon dioxide (also called silica). Silica has several crystalline structures (e.g quartz) and an amorphous structure. Silicon dioxide structure is amorphous, when produced through thermal oxidation. The crystalline structure is periodic in nature, extending over many molecules, while the amorphous has a non-periodic structure. Fig 2.2(b) is a two-dimensional schematic diagram of a quartz crystalline structure made up of rings with six silicon atoms. Fig 2.2(c) is a two-dimensional schematic

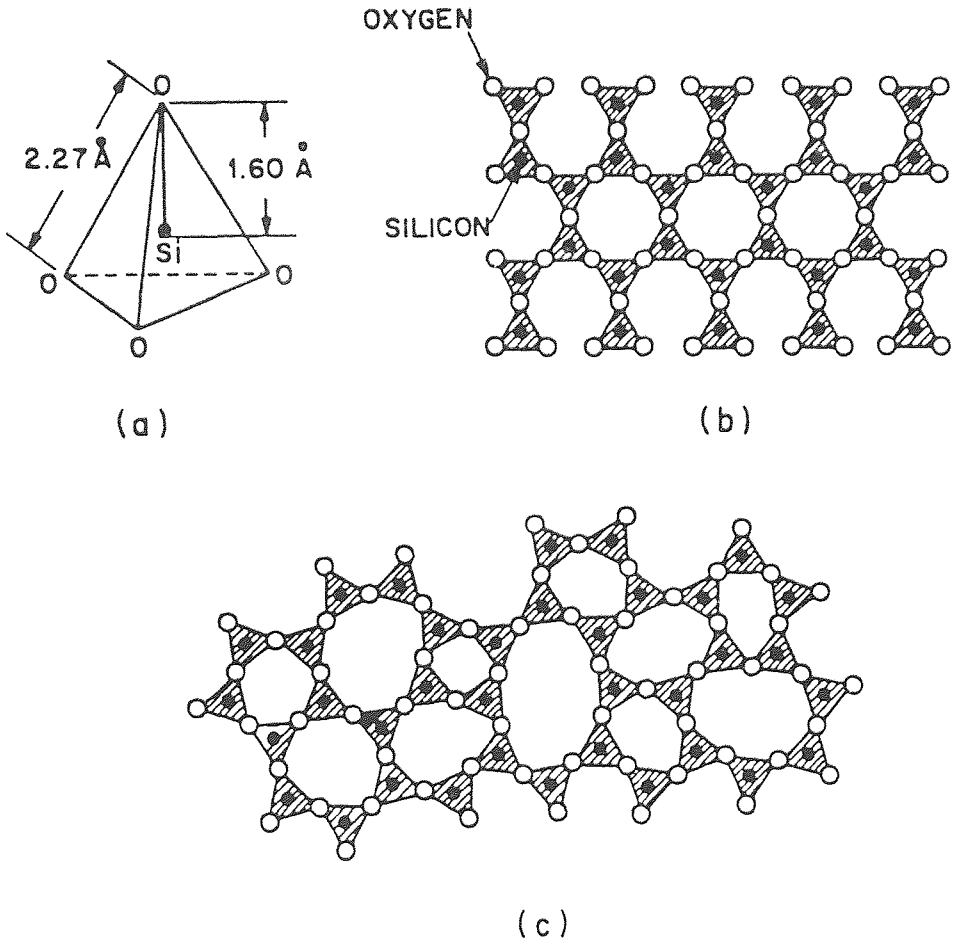


Figure 2.2: (a)Basic structural unit of silicon dioxide. (b) Two dimensional representation of a quartz crystal lattice. (c) Two dimensional representation of the amorphous structure of silicon dioxide[10].

diagram of an amorphous structure for comparison. In the amorphous structure there is a tendency to form characteristic rings with six silicon atoms. It can be noted that the amorphous structure in Fig 2.2(c) is quite open because only 43% of the space is occupied by silicon-dioxide molecules.[10]

### 2.2.1 Oxidation Kinetics - Classical Theory

The macroscopic oxidation process was first suggested by Deal and Grove through a phenomological model developed by them. The model is schematically illustrated in Fig 2.3. This model is valid for oxide thicknesses above 300Å, oxidation in dry oxygen, oxidant partial pressure of 1 atm or less, and temperatures between 700 and 1300°C.

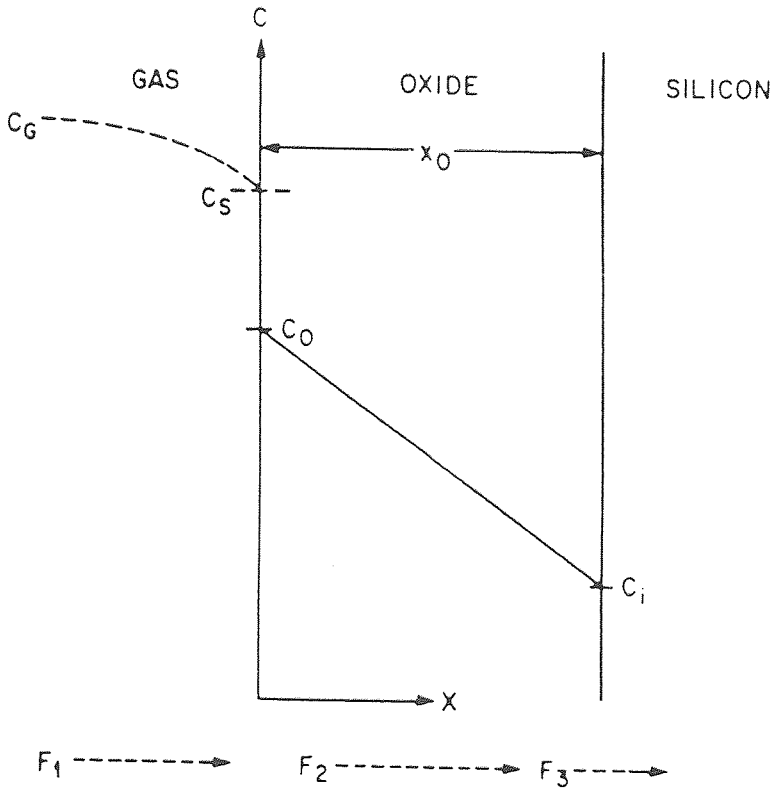


Figure 2.3: Cross section of silicon with a growing $SiO_2$ layer illustrating the model for thermal oxidation of silicon. The three fluxes, $F_1$ into the silica, $F_2$ through the silica, and $F_3$ at the Si-$SiO_2$ interface, are shown[6].

Let the silicon be covered initially by an oxide layer of thickness $x_o$, as shown in Fig 2.3. The overall process is divided in three consecutive stages :

(1) Molecules from the oxidant are transported from the gas atmosphere to the outer surface of the already formed oxide layer, through the gas-oxide interface with flux $F_1$. (Flux is defined as the number of atoms or molecules crossing a unit area per unit time). As the gas-phase mass-transfer coefficient is high, one can assume that the concentration of oxidant $C_o$ in the top layer of the oxide to be given by the equilibrium concentration of the oxidant at the oxidation temperature. It should be kept in mind that this equilibrium concentration of the oxidant in the oxide, $C^*$, i.e. the concentration in the oxide per cubic centimeter is linearly related to the partial pressure of the oxidant in the oxidizing gas by referring to Henry's Law and Ideal Gas laws

$$C_o = Hp_s \tag{2.3}$$

and,

$$C^* = Hp_g \tag{2.4}$$

where $p_s$, is the partial pressure in the gas adjacent to the oxide surface, $p_g$ is the partial pressure in the bulk of the gas, and H is Henry's law constant. Using Henry's law along with ideal gas law,

$$F_1 = h(C^* - C_o) \tag{2.5}$$

(2) The oxidant moves through the oxide layer towards the silicon surface. The diffusive flux of any part, x in the oxide layer is given by Fick's law,

$$F_2 = -D(\frac{dC}{dx}) \tag{2.6}$$

where, D is the diffusion coefficient and dC/dx is the concentration gradient of the oxidizing species within the oxide. The diffusion constant strongly depends on the structure (atomic, molecular or ionic) of the oxidant. Under steady state conditions, $F_2$ is constant throughout the oxide layer and a linear concentration profile is obtained. This means that $F_2$ is also given by,

$$F_2 = D\frac{(C_o - C_i)}{X_o} \tag{2.7}$$

where, $C_i$ is the concentration of oxidation at $Si$ - $SiO_2$ interface.

(3) The oxidant reacts at the Silicon surface to form a new layer of Silicon dioxide. The rate of this interface reaction is assumed to be proportional to the oxidant concentration at the interface, so that the resulting flux $F_3$ becomes,

$$F_3 = K_s C_i \tag{2.8}$$

where, $K_s$ is the chemical surface-reaction rate constant for Silicon oxidation.

Under steady state conditions, the fluxes $F_1$, $F_2$ and $F_3$ must be equal and solving the two simultaneous equations, $F_1$=$F_2$ and $F_2$=$F_3$, expressions for $C_i$ and $C_o$ can be obtained. Thus,

$$C_i = \frac{C^*}{1 + \frac{K_s}{h} + \frac{K_s x_o}{D}} \tag{2.9}$$

and,

$$C_o = \frac{(1 + \frac{K_s x_o}{D})C^*}{1 + \frac{K_s}{h} + \frac{K_s x_o}{D}} \tag{2.10}$$

There are two limiting cases, which may arise, when the diffusivity is either very small or very large ( i.e $D \gg K_s x_o$ ) so that from eqn (2.9) and eqn (2.10), $C_i \rightarrow 0$ and $C_o \rightarrow C^*$. This case is called the diffusion-controlled case, because the diffusion flux, governed by D, becomes small compared to Silicon surface reaction flux governed by $K_s$. Here the rate of oxidation is limited by the availability of oxidant at the Si-$SiO_2$ interface, and the oxidation rate is controlled by the reaction rate constant, $K_s$ and by $C_i$ (which equals $C_o$).

Substituting eqn (2.9) into eqn (2.8), the flux of oxidant reaching the Si-$SiO_2$ interface is

$$N_1 \frac{dx_o}{dt} = F_3 = \frac{K_s C^*}{1 + \frac{K_s}{h} + \frac{K_s x_o}{D}} \tag{2.11}$$

The solution of this differential equation subject to boundary conditions that an oxide may be present initially from previous processing steps or may grow before the assumptions in the model are valid, that is $x_o = x_i$ at t = 0 is,

$$x_o^2 + A x_o = B(t + \tau) \tag{2.12}$$

where,

$$A = 2D[\frac{1}{K_s} + \frac{1}{h}] \tag{2.13}$$

$$B = \frac{2DC^*}{N_1} \tag{2.14}$$

and,

$$\tau = \frac{x_i^2 + A x_i}{B} \tag{2.15}$$

The quantity $\tau$, represents a shift in the time co-ordinate to account for the presence of the initial oxide layer $x_i$.

*Equation 2.12 is the general relationship for thermal oxidation of Silicon* [11, 13].

Solving the quadratic relationship of Eqn. 2.12 for $x_o$ as a function of time $t$, we obtain,

$$\frac{x_o}{A/2} = (1 + \frac{t+\tau}{A^2/4B})^{1/2} - 1 \tag{2.16}$$

There are two limiting cases of eqn 2.12. For long oxidation time (i.e thick oxides) when $t \gg A^2/4B$ and $t \gg \tau$, eqn 2.13 becomes,

$$x_o^2 = Bt \tag{2.17}$$

Equation 2.17 is called the *parabolic law* and $B$ is called the *parabolic rate constant.* This limiting case is the diffusion-controlled case (discussed previously).

For short times (i.e thin oxides) when $(t + \tau) \gg A^2/4B$, eqn 2.13 becomes,

$$x_o = \frac{B}{A}(t + \tau) \tag{2.18}$$

This reaction is called the linear law and the quantity B/A is called the linear rate constant. This case is the reaction controlled case, discussed previously.

The general oxidation equation is a good fit for thick oxides and oxidation in wet oxidizing atmosphere, but for dry oxidation, the fit of eqn 2.12 to the oxidation data does not extrapolate to zero initial thickness but instead to a value that equals about 250$\mathring{A}$, for data spacing a range of 700 to 1200°$C$. As stated before, Deal and Grove found, in fact, that there was an initial accelerated growth during oxidation in dry $O_2$.

A number of different forms and mechanisms have been suggested for the initial thin oxide growth relationship. The proposals in the literatures have included schemes based on enhanced oxidant diffusion, reduced oxidant diffusivity in the oxide, fixed charge effect on the interface reaction rate and micropore diffusion [14]. Rather than surveying the various possibilities here, the thesis aims at reviewing the current models and arrive at the best possible relationship in the light of the available experimental data. The next section is devoted to explain, some of the possibilities, which might account for the oxidation mechanism.

## 2.3 Oxidation Mechanism

### 2.3.1 Atomic Reactions

As indicated in Section 2.2.1, the thermal oxidation of Silicon in either dry oxygen or steam can be characterized by the general relationship equation 2.12. However the actual atomic reactions at the Si-$SiO_2$ interface during thermal oxidation have not been well understood in the past. More recently, efforts have been made to characterize these reactions, especially the mechanism associated with the rate constant $K$ in eqn. 2.12. It has been proposed that at least three individual phenomonea occur at the Si-$SiO_2$ interface as oxidation proceeds [15]. These are shown in Fig. 2.4.

Firstly each $SiO_2$ molecule produced occupies considerably more volume than that of Silicon reacted. Thus appreciable strain results at the interface region as is indicated by the upper box in the Fig 2.4. This compressive stress accounts in part of the excellent passivation property of thermal Silicon Oxide, but can also lead to lattice mismatch and other defects, if some mechanism does not permit the stress to be relieved.

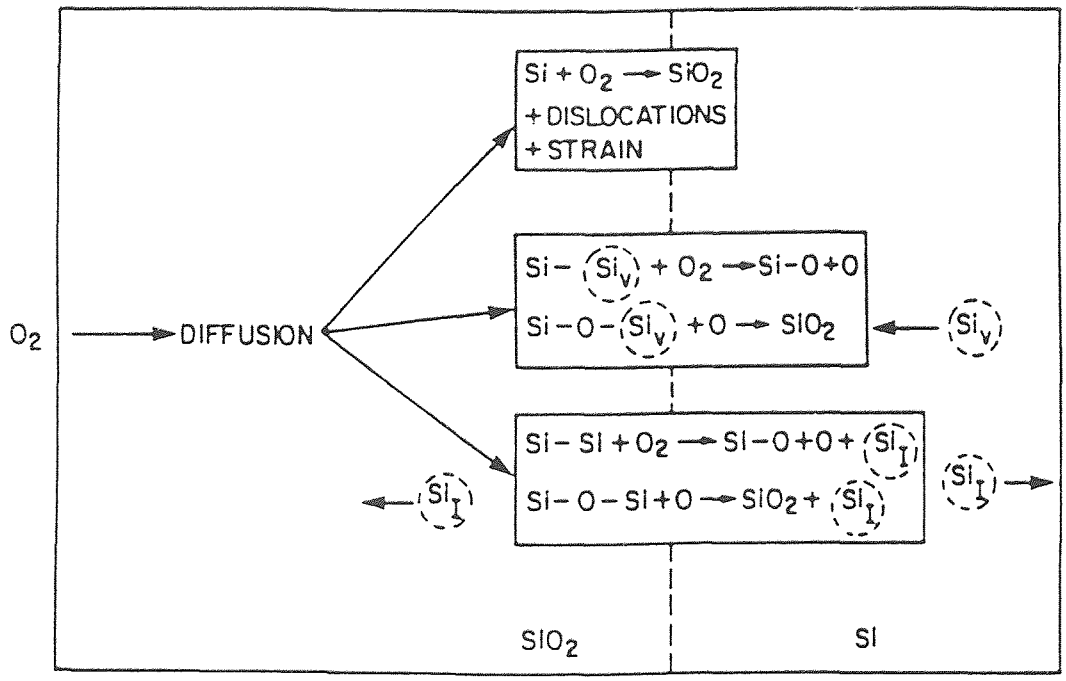


Figure 2.4: Proposed Mechanism occuring at Si-$SiO_2$ interface during Silicon Thermal Oxidation[15].

One of the ways of relieving this stress is shown in the lower box of Fig 2.4, which is the generation and diffusion away from the interface of Silicon interstitials. Silicon interstitials are produced by the oxidation process have been proposed to cause enhanced diffusion of dopants in the Silicon during thermal oxidation - OED(oxidant enhanced diffusion) as well as to promote stacking fault formation - OISF(oxidation induced stacking fault). It has been proposed that they contribute to charges such as $Q_F$ (Fixed oxide charge) or $Q_{it}$ (Interface trapped charge) in the oxide. For the enhanced dopant diffusion effect, a relationship relating the oxidation rate and effective diffusion coefficient has been developed, which agrees reasonably well with experimental data :

$$D_{eff} = D_i + K[\frac{dx}{dt}]^n \tag{2.19}$$

where, $D_i$ = the normal diffusion coefficient due to vacancy mechanism and $K(dx/dt)^n$ = Silicon interstitial contribution. The value of $n$ has been determined to range from 0.2 to 1.0. An expression for stacking fault, generation and retrogrowth has also been proposed :

$$\frac{dl}{dt} = K_1[\frac{dx}{dt}]^n - K_2 \tag{2.20}$$

where, $\frac{dl}{dt}$ = growth/retrogrowth rate, $K_2$ = the shrinkage rate in the absence of oxidation and $K_1(dx/dt)^n$ = the interstitial contribution to the growth rate. A number of process variables in addition to oxidation rate dx/dt, such as ambient type, silicon orientation, HCl presence and mechanical damage have been shown to affect oxidation-enhanced diffusion and stacking fault generation through the formation of Silicon interstitials during oxidation.

The third reaction or mechanism proposed to occur at the Si-$SiO_2$ interface,

indicated by the middle portion of Fig. 2.4, involves the possible contribution of Silicon vacancies to the oxidation reaction. Under normal conditions (lightly doped Silicon) the vacancy concentration is reasonably low and oxidations proceeds giving rise to the mechanism, already discussed (strain generation and silicon interstitial effects). However, for heavier dopant concentration ( $C_B = \geq 10^{20} cm^{-3}$) enough silicon vacancies are present so as to provide additional free volume which can accommodate additional interstitials and as a result, the oxidation rate increases [15].

An understanding of the detailed mechanisms of reactions occuring at the Si-$SiO_2$ interface during thermal oxidation, such as those described above, and the relationship to associated reactions occuring during the oxidation process,should provide the basis for producing and controlling the thin oxides required for VLSI circuits.

# Chapter 3

# Oxidation Techniques

## 3.1 Introduction

In this chapter, the most commonly used techniques for thermal oxidation of silicon will be discussed, and some equipment and processing related consider ations will be made.

From a practical point of view, thin oxide growth must be slow enough to obtain uniformity and reproducibility. Various growth techniques include dry oxidation, dry oxidation with HCl, sequential oxidations using different temperatures and ambient, wet oxidation, reduced pressure techniques and high pressure/low temperature oxidations. The oxidation rate will, of course, be lower at lower temperatures and at reduced pressures. Ultra-thin oxides($< 50\mathring{A}$) have been produced using very hot nitric acid, boiling water, and air at room temperatures. New thin

oxide growth techniques have also recently been developed using Rapid Thermal Oxidation (RTO).

This chapter will give an overview of the thin oxide growth techniques as well as the different oxidation techniques and its implementation, alongwith with the procedures for measurement of oxide thicknesses.

## 3.2 Thin Oxide Growth Techniques

Much work has been done to achieve uniform, thin oxides under controlled processing conditions. In order to *controllably* grow thin oxides, the growth rate must be reduced so that the process entails a reasonable time of growth. Various techniques have been used to achieve this reduced growth rate. They include :

a) Dry oxidation

b) Dry oxidation with HCl, trichloroethylene(TCE) or, trichloroethane (TCA)

c) Reduced pressure oxidation

d) Low temperature, high pressure oxidation

e) Rapid thermal processing(RTP) under oxidizing conditions.

Thin oxides ($\leq 400\mathring{A}$) have been successfully grown by a number of methods. Irene [16] has grown thin oxides ($\leq 200\mathring{A}$) in the temperature range of $780 - 980°C$ dry $O_2$. He reported that controlled oxides of $100\mathring{A}$ could be grown in 30 mins. at $893°C$. Adams,*et al.*, described the growth of thin oxides prepared in LPCVD system at reduced pressures (0.25 - 2 Torr) in the temperature range of $900-1000°C$. It was found that the properties of the oxides were comparable to those grown at 1 atm, but with the additional benefit of excellent thickness control down to $30\mathring{A}$. Oxides grown at higher pressure (10 atm) and low temperatures ($750°C$) have produced $300\mathring{A}$ films in 30 minutes. When these films were used as gate oxides in NMOS devices (DRAMs), the devices showed significantly improved refresh cycle

times [18] when compared with devices with films grown at 1 atm. Rapid Thermal Oxidation (RTO) performed in a controlled oxygen ambient with heating produced by tungsten-halogen lamps [13] have also produced oxides with good uniformity and breakdown field. Oxides of $40 - 130\mathring{A}$ ($1150°C$, 5 to 30 seconds) with breakdown fields of 13.8 MV/cm for $100\mathring{A}$ oxides has been produced with this method. More recently it has also been announced (AG Associates) that RTP has produced oxides in the range of $50 - 250\mathring{A}$ having well controlled thickness and electrical properties. Another more complicated technique utilizes ultraviolet pulsed laser excitation in an oxygen environment.

## 3.3 Processing Techniques

The processing techniques have an important impact on oxide properties. It has been noticed by some researchers that oxide density[19] increases as the oxidation temperature is reduced. Additionally, HCl ambients have typically been used to passivate ionic sodium, improve the breakdown voltage, and gather impurities and defects in the Silicon.

The oxidation technique chosen depends upon the thickness and oxide properties required. Oxides that are relatively thin and those that require low charge at the interface are typically grown in dry oxygen. When Sodium ion contamination is of concern, $HCl - O_2$ is the preferred technique as mentioned above. Where thick oxides (i.e $> 0.5\mu m$) are desired, steam is used ($\sim$ 1 atm or an elevated pressure up to 25 atm). Higher pressure allows thick oxide growth to be achieved at moderate temperatures in reasonable amounts of time.

### 3.3.1 Pre-Oxidation Cleaning Procedure

Before putting the Silicon wafers in an oxidation furnace, they are thoroughly cleaned in order to remove all traces of organic materials and/or metallic impurities, arising from previous processing steps and handling. Such contamination, if not removed, can degrade the electrical characteristics of the devices and can contribute to reliability problems.

Particulate matter is removed by either mechanical or ultrasonic scrubbing. Immersion processing techniques were the preferred cleaning methods, until the development of centrifugal spray methods, which eliminate the building up of contaminants as cleaning progresses. The chemical cleaning procedure usually involves removing the organic contamination, followed by inorganic ion and atom removal.

A typical cleaning procedure is the so-called *RCA Cleaning* in which hot aqueous solutions of $H_2O - H_2O_2 - NH_4OH$ and $H_2O - H_2O_2 - HCl$ are used to remove respectively, the organic and heavy metal contamination. The former solution acts by the solvating action of ammonium hydroxide and the oxidizing effect of the peroxide. This process can also complex some Group I and Group II metals. The latter solution prevents replating by forming soluble complexes with the removed ion, and the process is performed between 75 and $85°C$ for 10 to 20 minutes, followed by a quench, rinse, and spin dry[13]. It is also noticed that during most wafer cleaning procedures, a chemical $SiO_2$ layer of about 2 - 3 nm is formed. This oxide can be stripped in a diluted (e.g 5%) HF bath, followed by an extended rinse in a continuous flow of deionized water. Prolonged exposure of the bare silicon wafers to air also leads to the growth of a thin native oxide. It should be clear that reproducible growth of thin oxides requires careful control of the overall wafer handling before oxidation. Furthermore it has been reported that the cleaning

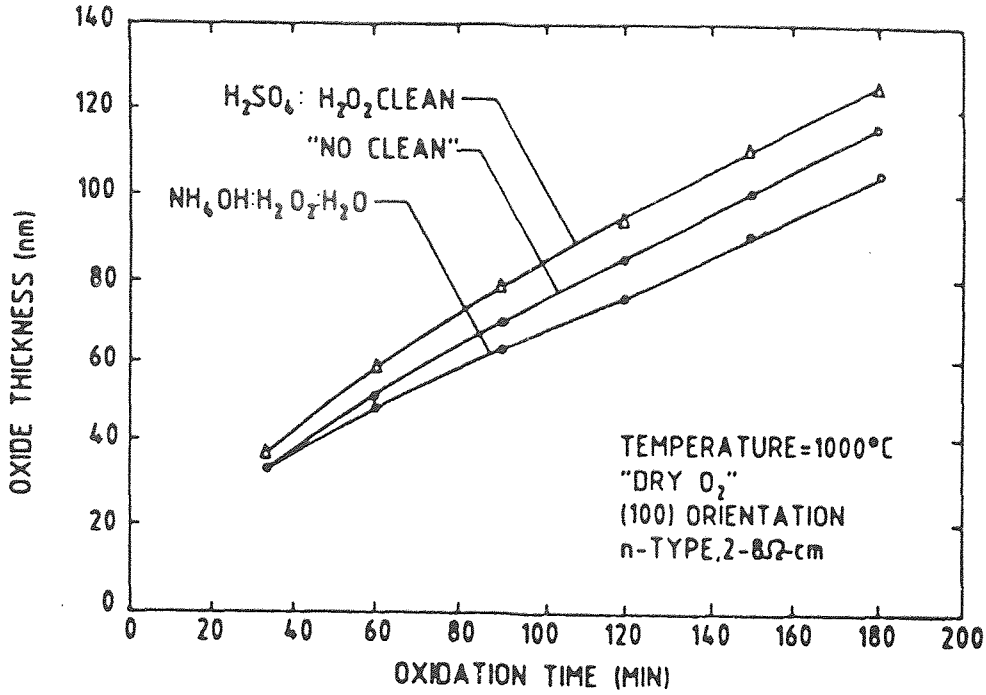


Figure 3.1: The effect of the pre-oxidation cleaning procedure on the oxidation rate [20]

procedure itself has an effect on the oxidation kinetics as illustrated in Fig 3.1[20]. Wafers taken from the container as supplied by the Silicon vendor and indicated by "no clean" showed a considerable thinner oxide than wafers treated in a Sulfuric-peroxide mixture before oxidation. On the contrary, wafers cleaned in an ammonium hydroxide - peroxide mixture gave a somewhat thinner oxide.

### 3.3.2 Dry or Wet Oxidation

As already mentioned in Chapter 2, most of today's oxidation process are carried out at atmospheric pressure in oxidation furnaces. Thin gate oxides are very often grown in dry oxygen for reasons of reproducibility and oxide quality. Recently a lot of attention goes to the use of double-walled quartz tubes, allowing to maintain

a flow of oxygen with a small amount of HCl or another chlorine additive between inner and outer tube. Thicker or less demanding oxide layers such as field oxides or masking layers are mostly produced in a wet or steam ambient. To obtain a wet oxidation atmosphere, oxygen is bubbled through deionized water kept at $95-97°C$. However, as the water bubblers easily get contaminated, wet oxides very often suffer from stability problems. To overcome this problem, it has been suggested to use a mixture of $O_2$ and $H_2$ gas to form water vapor in the oxidation tube. In practice, hydrogen is injected in the oxygen stream at the gas inlet of the furnace. These "hydrox" oxides are very stable under elevated temperature and bias conditions.

### 3.3.3 Chlorine Oxidation

The addition of chlorine containing additives to the oxidizing gas, has found widespread use for a number of reasons, related to oxide quality. Many production lines use HCl, which can be fed directly into the furnace tube. However if stainless steel tubing is used, great care should be taken to avoid contamination of the HCl with traces of $H_2O$. This indeed would lead to a very corrosive mixture, which is known to severely attack the tubing system. For the same reason, a small leak in the HCl gas system will also damage the surrounding equipments. This problem can be overcome by using a liquid chlorine compound like trichloroethylene (TCE) or 111-trichloroethane (TCA, also called $C_{33}$). For safety reasons, TCA has been given the preference. Prolonged contact to TCE can lead to liver, kidney and heart injuries.For the sake of completeness, it should be reminded here that the addition of 1% TCA to the oxidizing ambient corresponds to the addition of 3% HCl[21]. One should also be aware that very small concentrations of phosgene ($COCl_2$) can be formed when the reacted gases reach the cold end of the furnace tube. Hence an efficient exhaust system is mandatory when chlorine containing compounds are

used.

### 3.3.4 High Pressure Oxidation

Thermal oxidation of Silicon at pressures higher than 1 atm. have received considerable attention over the last years, as it offers a technique to grow thermal oxides at lower temperatures and at faster rates than can be achieved by means of conventional oxidation at atmospheric pressure. This interest has to do with the general trend towards lower temperature processing, required to reduce dopant diffusion and to maintain shallow junctions needed in VLSI processing. Another advantage is that oxidation-induced defects are suppressed. For higher-temperature, high pressure oxidation, the oxidation time is reduced significantly.

The oxidation is in principle done inside a quartz reaction vessel, which is surrounded by a nitrogen-containing region within the outer pressure shell. The pressure in the quartz tube can be as high as 25 atm. The high-pressure technique has been used mostly in bipolar applications, although some companies have applied it to MOS products. Fig 3.2 shows oxide thickness versus time data [22] for steam oxidation at various pressures and $900°C$. The substantial acceleration in the oxidation rate caused by the increased pressure is apparent.

### 3.3.5 Plasma Oxidation

The anodic plasma-oxidation process offers the possibility of growing high quality oxides at temperatures even lower than those achieved with the high-pressure technique[13]. This process has all the advantages associated with low-temperature processing, such as minimized movement of previous diffusions and suppression of defect formation. Anodic plasma oxidation can grow reasonably thick oxides (of the order of $1\mu$m) at low temperatures ($< 600°C$) at growth rates up to about $1\mu$m/h.

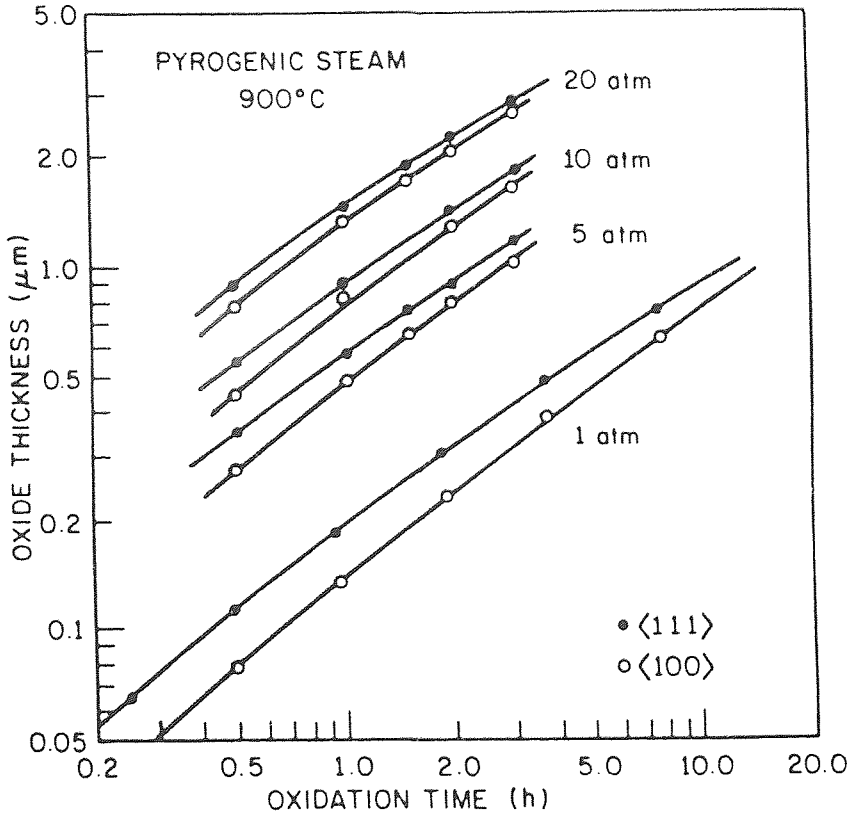


Figure 3.2: Oxidation thickness versus oxidation time for pyrogenic steam at 900°C for <100> and<111> Silicon and pressures upto 20 atm.

Plasma oxidation is a low-temperature vacuum process, usually carried out in a pure oxygen discharge. The plasma is produced either by a high-frequency discharge or a DC electron source. Placing the wafer in a uniform density region of the plasma and biasing it positively below the plasma potential allows it to collect active charged oxygen species. The growth rate of the oxide typically increases with increasing substrate temperature, plasma density, and substrate dopant concentration.

### 3.3.6 Other Oxidation Techniques

A variety of new techniques is being explored in order to grow high quality thin Silicon dioxide layers in a reproducible way. The use of double walled oxidation tubes was already mentioned in Section 3.3.2 has beneficial effect on the breakdown characteristics of the oxides.

The reduced pressure oxidation (0.25 - 2.0 Torr) by Adams *et al.* in a low pressure reactor at $900 - 1000°C$ lead to a good control of the thin oxide growth

due to lower oxidation rate.

It is also interesting to note that two-step process have been proposed to take full advantage of the HCl oxidation technique[23]. First a low temperature oxidation, resulting in a good control of the oxide thickness, is performed in a chlorine-containing ambient. The oxide is then annealed at a higher temperature in a mixture of $N_2$, HCl and $O_2$ in order to improve oxide quality without losing control over oxide thickness. Such oxides were shown to have reduced defect density.

## 3.4 Implementation

In industrial practice today, silicon dioxide films are grown in a reactor such as that illustrated in Fig. 3.3. The reactor consists of a resistance heated furnace held at a temperature around $1000°C$ by a temperature controller, a cylindrical fused quartz tube in which the silicon wafers are placed, and a source of either dry oxygen or pure water vapor. In production furnaces, temperatures can be held for short times(days) to within $\pm 0.1°C$ over the length of the flat zone (up to 2 ft long), and for long terms (months) to within $\pm 0.5°C$.

The loading end of the furnace tube protrudes into a vertical laminar flow (Whitfield) hood where a filtered flow of air is maintained. Flow is in the direction of the arrows shown in Fig 3.3. The purpose of the hood is to reduce dust and particulate matter in the air surrounding the wafer to negligible levels. Such particulate matter is undesirable because it can adhere, by electrostatic forces, to the silicon wafers prior to oxidation and contaminate either the oxide layer subsequently grown on the underlying silicon. Sodium contamination which is very critical from the point of device characteristics and supposed to be produced from furnace lining is minimized by the furnace manufacturer in the type shown in Fig 3.3.

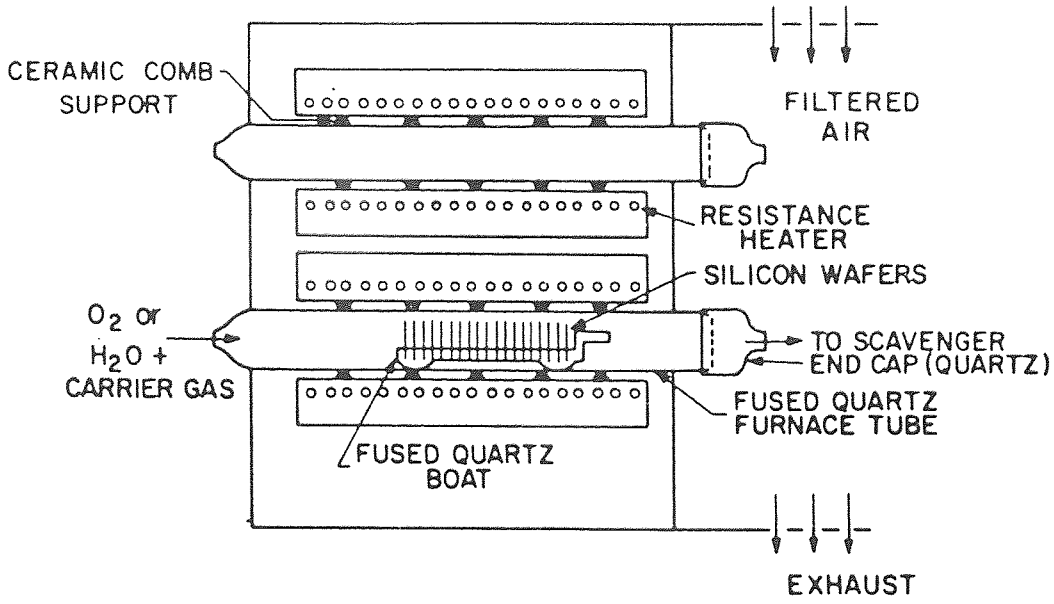


Figure 3.3: Schematic cross section through a stack of two resistance heated oxidation furnaces. The silicon wafer loading area is shown in a Whitfield-type hood

Gases coming out of the furnace during oxidation are not exhausted into the Whitfield hood but are passed through a scavenger (not shown in Fig. 3.3) and then exhausted into the atmosphere. The scavenger is made up of stainless steel or coated with Kynar to retard corrosion. When anhydrous HCl or $Cl_2$ is mixed with oxygen, which is sometimes done to produce sodium free oxides, the exhaust gases flow through a water spray scrubber, to remove chlorine from the gas stream by forming HCl.

Distilled water, or deionized water passed through filters to remove particulate matter and organics are the sources of steam or water vapor for wet oxidation. To prevent room air (which may contain impurities that adversely affect film quality) from entering the oxidation zone, the ambient gases in the furnace tube are held at a pressure just slightly above 1 atm. The oxidant gas flows at the rate of about 1 cm/sec past the wafers in the furnace at oxidation temperature.

For growing wet oxides, water vapor can be steamed at slightly above 1 atm or

can be mixed with a neutral gas like argon. The use of carrier gas provides better thickness control because growth is slower.

Most modern furnace systems utilize either microprocessors or minicomputers to control the operation of the furnace. The desired insertion and withdrawal rates, ramp rates, gas flows, and temperatures are all programmable. For wet oxidation the microprocessor controls the $H_2/O_2$ mixture.

## 3.5 Latest Trends

As VLSI devices continue to be scaled-down in size, they will require gate and tunnel dielectric thicknesses in the range of 100$\mathring{A}$ or less. In spite of the fact of that very thin oxides can be grown by a number of techniques as described in the preceeding sections, very thin layers of $SiO_2$ are known to have high defect densities, and do not serve as an effective diffusion mask against impurity diffusion.[18] Recent studies show that direct *thermal nitridation* of Si and thin $SiO_2$ appears to be a viable alternative method of growing a good quality dielectric film in this very thin regime.

Thermally grown films of *silicon nitride* ($Si_3N_4$) have a number of advantages over $SiO_2$, easily including :

a) they tend to have self-limiting growth kinetics and therefore their thickness is easily controllable

and, b) they are effective barriers to impurity diffusion.

MOS devices fabricated with these films show large values of gain.

Thermal silicon nitride films are generally grown by the high temperature ($950 - 1200°C$) nitridation of silicon in pure ammonia ($NH_3$) or an ammonia plasma [18]. They can also be prepared by plasma anodic nitridation using a nitrogen-hydrogen plasma in the temperature range of $700 - 900°C$. An additional and somewhat

novel technique for producing nitride films on silicon is to use direct nitrogen ion implantation at a dose of $5X10^{16}cm^{-2}$, in the energy range of 5-60 KeV, followed by an anneal at $1000^{o}C$, in a $N_2$ ambient.

## 3.6 Measurement Techniques

The accurate measurement of oxide film thickness is an important process control tool used during VLSI wafer fabrication. For example, the thickness of gate oxides in VLSI MOS devices (which is typically $\leq 250\mathring{A}$) must be tightly controlled, as it is one of the parameters that directly determines the device threshold voltage, $V_T$. Various techniques are available for measuring oxide thickness, the most important being :

a) Optical interference

b) Ellipsometry

c) Capacitance

d) Use of Color chart

All the above are non-destructive optical techniques. Since, ellipsometry is employed in this research, a brief idea of the method is described below.

The ellipsometry technique makes use of the change of state of the polarization of light when it is reflected from a surface (in this case the oxidized $Si/SiO_2$ interface). The state of polarization is determined by the relative amplitude of the parallel and perpendicular components of the radiation, and by the phase difference between these two components. The polarization change depends on the optical constants of the silicon, the angle of incidence of the light, the optical constants of the film (i.e $n_i$ and the extinction coefficient, k), and the film thickness. If the optical constants ($n_i$, k) of the substrate are known and the film is non-absorptive at the wavelength being used (k = 0), the state of polarization of the reflected beam depends on $n_i$

and the thickness of the transparent film.

High Resolution Electron Microscopy (HREM), is also a powerful technique in characterizing very thin oxide films. In this research, Transmission Electron Microscopy (TEM) has been employed. It was quite interesting to note the discrepancy between the ellipsometric measurements and that obtained by TEM. This poses a question regarding the reliability of ellipsometric measurements. This is further discussed in Chapter 6.

# Chapter 4

# Existing Models - in the thin oxide regime

## 4.1 Introduction

Extensive research efforts have been employed to model the oxidation kinetics of silicon in the thin oxide regime. It is already described in Chapter 1, that the oxidation of single-crystal silicon is, for the most part, accurately characterized by the Deal-Grove formalism[6]. Many authors, however, have reported considerable deviation from the linear-parabolic oxidation theory when the thin oxide films are grown in a dry oxygen ambient. The deviation from this model consists of anomalously rapid initial oxidation for the first 20-40 nm of growth in dry $O_2$. The standard linear-parabolic formulation accounts for this regime empirically by the incorporation of a time constant $\tau$ in the expression for oxide growth.

A wide variety of functional relationships have been proposed. In this section several possibilities are considered in light of oxide thickness data obtained by ellipsometry and HRTEM.

## 4.2 Background

The oxidation of silicon appears, at first, to be a simple problem. Oxygen reacts with the surface layer, with reaction continuing at the interface between the substrate silicon and the oxide as the film grows in thickness. Oxygen must diffuse in through the film to reach the interface.

Although the basic situation is summarized in these simple statements, the number of complicating factors and difficult issues is disturbingly large. A number of the questions that are relevant to a study of this anomalously rapid initial regime are listed below.

- Does oxygen diffuse through the oxide in molecular or atomic form ? If it diffuses molecularly, does the interface reaction involve the molecular form or is dissociation required prior to reaction?

- Is the transported oxygen a charged species? If not, is an ionization reaction necessary at or near the interface?

- Is there, in fact, a single oxidant species, or do several species simultaneously make a significant contribution to diffusion and/or interface reaction?

- Is the rapid oxidation a diffusion-controlled phenomenon or an interface-controlled one?

- The oxidation of silicon to form silicon dioxide requires a large volume change (per silicon atom). Large planar stresses are generated. What are the effects of these stresses? Are they capable of giving rise to the observed growth rate enhancement?

- Silicon interstitials are likely to be released at the surface, and vacancies in the

silicon consumed there. How do these point defects relate to initial oxidation?

Some of these questions have clear answers; most do not. The major diffusing species for thicker oxides is almost certainly molecular oxygen, as inferred from the pressure dependance of the parabolic rate constant and the agreement between the measured activation energy and that seen for $O_2$ molecules diffusing in fused silica. It had originally been thought that the application of an electrical potential across the oxide film affected oxidation rate, implying the involvement of ions. However, more recent works conclude that silicon oxidation is dominated by neutral species. The latter conclusion applies strictly to thicker oxides; the participation of charged species in the initial oxidation has not yet been ruled out[14].

Although oxide films grown above the viscous flow point of silicon ($950 - 975°C$) appear to remain stress-free during oxidation, thermal growth of $SiO_2$ at lower temperatures, does give rise to larger compressive stresses in the oxide[24]. However the effect of stress on diffusion or on the interface reaction are still unclear. The role of point defects has also not been elucidated in the early stages of oxidation. Many of the other mechanisms in this list have been invoked to explain or model the rapid initial oxidation. It is disconcerting to realize that sometimes the assumption of the same model has led to dissimilar expressions for oxide growth.

In this research, the various models are categorized by the functional forms that they give rise to for the initial oxidation regime. The different forms considered by the former researchers are listed below :

$$x = A_o + A_1 t + A_2 t^2 (Linear - Parabolic) \tag{4.1}$$

$$x = A_o + A_1 t (Linear) \tag{4.2}$$

$$x = A_o + A_1 x^2 (Parabolic) \tag{4.3}$$

$$x = A_o t^{A_1} (VariableePower) \tag{4.4}$$

$$x = A_o + A_1 lnt (Logarithmic) \tag{4.5}$$

$$1/x = A_o + A_1 lnt (InverseLogarithmic) \tag{4.6}$$

$$x = A_o + A_1 t^{1/3} (Cubic) \tag{4.7}$$

In these equations. $t$ represents oxidation time, $x$ is oxide thickness, and $A_o, A_1$ and $A_2$ are fitting constants that may or may not be thermally activated or pressure dependant. Although several models may give rise to similar expressions, it should be possible to at least eliminate some of the alternatives by determining what functional form the data follow.

### 4.2.1 Linear modeling of initial oxidation

There are numerous reports that the early regime of rapid oxidation in dry $O_2$ can be well fit to a linear relationship. In some of these cases, the initial growth is considered to be the linear part of the Deal-Grove description which is controlled by the interfacial reaction rate and governed by the linear rate constant B/A (sometimes also designated by $K_{lin}$). This implies a more gradual and perhaps more complex transition between the linear and parabolic kinetics than that proposed by Deal and Grove[6]. Other formulations give rise to an initial linear regime that precedes

the linear-parabolic behavior. Two separate linear rate constants corresponding to different physical processes are then obtained.

Growth kinetics for thin oxide layers on both (100) and (111) substrates were examined by Van der Meulen. The range of oxide thicknesses examined was restricted to 1-30 nm. Relatively low temperatures ($700 - 1000°C$) were used, and diluted ambients of dry $O_2$ in $N_2$ at 1 atm. total pressure were investigated. Wafer cleaning involved unspecified organic and inorganic rinses using ultrasonic agitation, following the procedures of Deal and Grove. The results obtained by him, were also characterized by a linear-time-thickness relationship that was thought to be the interface-controlled linear portion of the typical linear-parabolic growth. At the higher values of temperature and pressure that were examined, the transition to parabolic behavior was also evident for the thickest oxides measured. The linear rate constant data exhibited some curvature in an Arrhenius plot, prompting him to speculate that a complex interface reaction mechanism was necessary. From the pressure dependancies of B/A at different temperatures, it was suggested that the oxygen species involved in the rate-limiting step is not the same for the two orientations. A general expression for oxidation was obtained that consists of a mixed linear-parabolic expression with a logarithmic correction at large oxide thicknesses.

Irene appears to be the first to suggest that the initial rapid oxidation regime in dry $O_2$ is a separate linear region which is not encompassed by a linear-parabolic sort of description[16]. Oxidation kinetics in the initial linear region are described by an expression similar to eqn. 4.2. Wafers in his experiment were cleaned by RCA process and given a final HF dip and deionized water rinse. Data were collected during the early stages of oxidation in dry $O_2$ by automated *in-situ* ellipsometry, at oxidation temperatures of 780, 893, and $980°C$. Irene indicates that the presence of micropores in the oxide would provide an explanation for the initial rapid

oxidation behavior in dry $O_2$. Accelerated lateral diffusion of oxidants that were supplied directly to the silicon silicon dioxide interface via pores would result in linear kinetics.

Murali and Murarka's model incorporates an oxygen-diffused zone in the silicon substrate in the vicinity of the interface and predicts an initial linear region before the linear-parabolic regime[26]. They noted that in the early stages of oxidation, it is likely that oxidizing species are supplied to the interface more rapidly than they can be consumed by the interfacial reaction. As a result, excess oxygen will diffuse into the near-interface silicon to an extent determined by the oxygen diffusivity and solubility in silicon, oxygen partial pressure, temperature, orientation, and oxide thickness. A "reactive zone" is thus formed. Oxidation of silicon then occurs partially within this zone rather than entirely at the $Si - SiO_2$ interface.

### 4.2.2 Parabolic modeling of initial oxidation

The anomalously rapid initial oxidation has also been characterized by a parabolic expression. Experimental data that corresponded to a separate parabolic regime at oxide thicknesses under 12 nm were obtained by Adams, Smith and Chang[17]. Wafers of (100) orientation received an RCA type clean followed by a dilute HF etch and water rinse. Oxidations were performed at low oxygen pressures of 0.25-2.0 Torr of dry $O_2$ and at temperatures between $900°C$ and $1000°C$. The seven different rate laws listed earlier as Eqns. 4.1 to 4.7 were fitted to the oxide thicknesses measured by ellipsometry. The parabolic expression was determined to be the most appropriate representation. Linear, logarithmic, and inverse-logarithmic expressions followed the data poorly compared to the parabolic fit, and cubic and variable-power laws were discarded because there were no relevant physical mechanisms associated with them.

### 4.2.3 Linear-parabolic modeling of initial oxidation

In several cases, the initial anomalously-rapid oxidation regime has been modeled by another linear-parabolic expression. Adams et al.[17] examined the fit of their data to such an additional linear-parabolic equation (Eqn. 4.1) but determined that it provided only a marginally better description than a parabolic term alone, and that the slight improvement could be attributed solely to the presence of an additional fitting parameter. Both prior and subsequent work has been done that argues in favour of a separate complete linear-parabolic regime during early oxidation in dry $O_2$.

Extensive data on oxidation of (111) Si surfaces, alongwith some data on (100) surfaces, were collected in a relatively early study by Hooper et al.[27]. Samples were cleaned by the RCA method (discussed in Chap.3) with a final HF dip, but a subsequent $1200^{o}C$ treatment for 30 seconds in a high vacuum was instrumental in removing native oxide prior to thermal oxidation. Oxide growth was carried out at pressures from 50 to 1200 Torr (0.066 to 1.58 atm.) and at temperatures in the $650 - 950^{o}C$ range. Simple Deal-Grove kinetics or its modifications did not serve as appropriate descriptions of the thickness *vs* time data obtained from *in situ* ellipsometry. The linear-parabolic equation gave an excellent fit to the experimental data.

### 4.2.4 Variable-power law modeling of initial oxidation

A recent report by A. Reisman et al.[28] showed their data to be modeled accurately over a wide thickness range by the variable power law of the form given by Eqn. 4.4. Their study was conducted at $800^{o}C$ and 20 atm. in dry $O_2$ for (100) silicon. In each oxidation experiment, 25 wafers were oxidized, and twenty points were measured on each wafer, using an IBM film thickness analyzer. For the shorter time oxidations,

thicknesses were measured with an ellipsometer as well as the FTA. They actually proposed a general equation of the form given below :

$$x = a(t_g + t_o)^b \tag{4.8}$$

where, $x$ is the final measured thickness, $a$ and $b$ are constants, $t_g$ is the time for growth measured in an oxidation experiment, and $t_o$ is the time to grow an oxide of thickness $x_o$, already present on the silicon surface, and/or formed as a consequence of furnace ramp-up and ramp-down sequence. The values for $x_o$ and $t_o$ are determined readily from x-t data. Employing this model, they found that there is no evidence of *anomalous* oxidation region at small thicknesses. It was also found that all of the published data, including that published by Deal and Grove in 1965, could be modeled precisely and simply by the expression 4.8.

### 4.2.5 Other models in the initial regime

Of the other functional forms that have been advocated for explaining initial oxidation data, the most commonly mentioned possibility is the *inverse-logarithmic expression* (Eqn. 5.5). Although Deal and Grove did not specifically mention such a form, it was implicit in their speculation on the possible origins of the early growth rate enhancement in dry oxidation[12]. Rapid initial film growth is expected if an ionic species participates in the early stages of oxidation. If ionic transport does take place as suggested by them, very thin oxides will be grown approximately according to an inverse-logarithmic law.

Massoud et al.[29] have worked extensively in the thin oxide regime and it has been recently demonstrated by them that in the initial oxidation phase, a much better fit can be accomplished by adding an additional term to the oxidation rate stated by Deal and Grove, and which decays exponentially with thickness. The

expression formulated by them is shown below :

$$\frac{dx_{ox}}{dt} = \frac{B}{2x_{ox} + A} + C_2 e^{-x_{ox}/L_2} \tag{4.9}$$

where, $C_2$ is a pre-exponential constant and $L_2$ is a characteristic decay length. For dry oxidation of lightly doped substrates in the $800 - 1000^{o}C$ range, $L_2$ was found to be $70\mathring{A} \pm 10\mathring{A}$, independent of substrate orientation.

## 4.3 Summary

A detailed evaluation and discussion of the various physical models to explain the initial rapid oxidation phase, can categorize the models essentially into four groups[29].

(i) Models based on *space-charge effects* where the oxidation enhancement in the thin regime is due to field-assisted oxidant diffusion.

(ii) Models dealing with the presence of *structural defects in the oxide*, providing additional channels or micropores for diffusion of the oxidant.

(iii) *Stress effects* in the thin oxide can lead to a different diffusivity of the oxidizing species.

(iv) Increased solubility of the oxidant in the thin oxide could affect the growth rate by its influence on the oxidant concentration at the silicon surface.

Finally Massoud et al. proposed a new model based on the presence of a thin surface layer in the silicon where additional reaction sites are available. The concentration of these sites decays exponentially with a characteristic length of $\sim 40\mathring{A}$, corresponding with the $70\mathring{A}$ of oxide thickness observed for the characteristic length, $L_2$ in expression 4.10.

# Chapter 5

# Experimental Procedure

## 5.1 Introduction

Routine measurements of oxide thickness have been an integral part of silicon wafer for many years. Fabrication of thin film devices requires an accurate knowledge of both lateral and vertical film dimensions. Oxide thicknesses are commonly determined by nondestructive optical techniques such as interferometry and ellipsometry. For most purposes, these methods are sufficiently accurate. Very thin oxides, however, are more difficult to characterize by such measurements. The experimental data shown in the next section have been obtained earlier, using high-resolution transmission electron microscopy (HRTEM) and ellipsometry techniques.

In this chapter, the experimental methods, to obtain the above mentioned data, is discussed, alongwith the data analysis procedure adopted, to arrive at the best

model formulation.

## 5.2 Experimental Method

### 5.2.1 Pre-Cleaning and Oxide formation

The oxides were grown at $800°C$ on single crystal silicon wafers (p-type Czochralski). The wafer had an orientation of $< 100 >$ and $2\Omega - cm$ resistivity. The Silicon wafers were cleaned using conventional RCA technique (discussed in Sec 3.3.1) followed by a hydrogen fluoride (HF) dip and a thorough rinsing with deionized (DI) water. Oxides were thermally grown at the said temperature for time durations of 1 - 300 minutes. Ultra high purity oxygen ($H_2O$ < 0.5 ppm) was used in the oxidation process. Typically the oxide thickness used in the measurement of the electrical properties was ~20 nm. This thickness is typical of the present day gate oxides for a $1\mu$ CMOS process.

### 5.2.2 Measurements

Oxide thickness measurements were carried out using a carefully aligned Gaertner manual and automatic ellipsometer[1,12]. The agreement in the thickness obtained from both the ellipsometers was within 0.5 nm. Thickness measurement was carried out at nine position of the wafer. The mean deviation of the thickness was found to be $\sim$ 2%. For determination of the oxide thickness, a refractive index of 1.465 (at 632.8 nm corresponding to the He-Ne laser) for $SiO_2$ was used. In this technique, polarization angles of reflected light are measured and converted to film thicknesses. An important advantage of ellipsometry as a characterization technique, is that, it is non-destructive.

An automatic spectroscopic ellipsometer that has been built at Pennsylvania State University[30] was employed to perform SE on thin films of $SiO_2$ (on Si)

in the thickness range of 2 to 20 nm. EER studies were also made on some of this samples. For this purpose, each wafer was cut into 4 x 20 mm strips which were then used as test samples. An air tight quartz vessel was used to contain the non-aqueous electrolyte and test samples from which the light was reflected. A reference electrode was used to measure the actual potential causing the field across the sample. The non aqueous electrolyte consisted of a 0.1 molar solution containing a counter ion, tetrabutylammonium tetrafluoroborate, $[CH_3(CH_2)_3]_4NBF_4$ and a non conducting supporting electrolyte, acetonitrile $CH_3CN$. Cross-section samples of HRTEM were prepared using combination of mechanical and ion-beam polishing methods. High resolution phase contrast images of the interface were taken at Scherzer optimum defocus value of 65 nm and $< 100 >$ orientation using JEOL 200CX TEM at 200 KV with a 0.27 nm point to point resolution. The averages are arrived at by determining $t_{ox}$ at regular intervals across several micrographs and taking the mean of the measured values. For further details please refer to the published work [1,32].

## 5.3 Data Analysis

The analysis of data was done through a data analysis and graphics software, called GENPLOT[33]. The program has extensive analysis and data manipulation capabilities with curves and variables. It includes a very powerful set of data fitting routines. Data may be fit to a linear function (returning standard deviations and error estimates), polynomial functions (up to order 6), or to a user-specified arbitrary function. The last capability allows experimental data to be analyzed in terms of any analytic function of 10 or less independent variables. This non-linear fit searches the parameter space of these variables to obtain the best fit (in a least square sense) of the data to the analytic function. The best fit estimate and an

estimate of the error are returned to each parameter.

The powerful fitting routine which attempts to fit a user defined function to the experimental data, varying parameter in the function to minimize the least-squares deviation of the data from the function, is actually known as NLSFIT. The fits can be based on quantitative models.

In brief, NLSFIT takes a function and a set of variables upon which the function depends. The numeric value of each of these variables is then modified and the variance between the function and the data is determined. Using the change in the variance, a new guess is made for each of the variables, iterating through the parameter space until a sufficiently good minimum is located. In this search, NLSFIT evaluates the derivative of the fitting function with respect to each of the parameters at every point in the experimental data set. These derivatives may either be given analytically, or NLSFIT will determine them numerically. NLSFIT combines the gradient search and function linearization methods to minimize the number of steps required to converge to the best solution.

In essence, NLSFIT performs a n-dimensional search for the minimum of the variance function.

Residual Analysis is actually done by the following expression :

$$Error = \frac{1}{N}[\sum_{i=1}^{N}[f(t_i) - x_i]^2] \tag{5.1}$$

where, $N$ is the number of data points fitted, $f(t_i)$ is the user defined function and $x_i$'s are the experimental data points.

# Chapter 6

# Results and Discussion

## 6.1 Introduction

This chapter summarizes the experimental results obtained from ellipsometric and TEM measurements and also the data analysis performed on them, to arrive at the best possible model. The coefficients obtained from the fits are also presented for further interpretation.

Two questions that arise are : 1 - does the obtained fit model "dry" silicon oxidation in general, i.e, over a wide pressure-thickness-time matrix, and 2- what is the best analytical approach to modelling any specific set of data ? A third question which no attempt has been made to answer here is whether the expression also models steam silicon oxidation ?

## 6.2 Experimental Results and Discussion

A summary of the oxide thickness measurements is presented in Table 6.1. As can be seen from the table, the oxide thicknesses obtained by ellipsometry are within 1 nm of those measured by TEM.

Two very thin and two very thick samples (A through D) were chosen for HRTEM studies. Fig 6.1 shows the thickness versus time growth kinetics for these samples. From the figure it can be seen that the oxide growth data obtained from ellipsometry shows a non-linearity, whereas the data obtained from TEM is fairly linear. It may be noted here that the ellipsometry data of the oxide thickness in Table 6.1 and Fig. 6.1 represents an average of several nine-point measurements made on each wafer. The mean deviation of the oxide thickness was found to be within 0.3 nm.

Similar measurements of the oxide thickness in the thin oxide regime have been recently reported by Carim[14]. It is interesting to note that our results of the growth rate behavior obtained from TEM and ellipsometry are similar to those reported by them despite the major differences in the method of growth of the oxide in two cases. In the present study, the oxides have been grown at $800^oC$ in dry $O_2$, while they grew [14] the oxides at $900^oC$ in an ambient of 10% dry $O_2$ in Ar.

In this discussion, the various models are categorized by the functional forms, that they give rise to for the initial oxide regime. Separate linear, parabolic, linear-parabolic, and variable power forms have been used to characterize the initial oxidation preceding the linear-parabolic portion of the curve that is well described by the Deal-Grove equation. The expressions 4.1 through 4.4 are considered in the work.

| SAMPLE | OXIDATION TIME (T) (MINS) at 800$^0$C | OXIDE THICKNESS (X) | |
|---|---|---|---|
| | | ELLIPSOMETRY (nm) | HRTEM (nm) |
| A | 1 | 2.0 | 3.0 |
| | 5 | 3.1 | |
| B | 10 | 3.7 | 3.5 |
| | 20 | 5.2 | |
| | 40 | 6.7 | |
| C | 100 | 10.8 | 9.5 |
| | 200 | 16.6 | |
| D | 300 | 21.3 | 22.0 |

Table 6.1: Summary of the oxide thickness measurements. All thickness represent average values

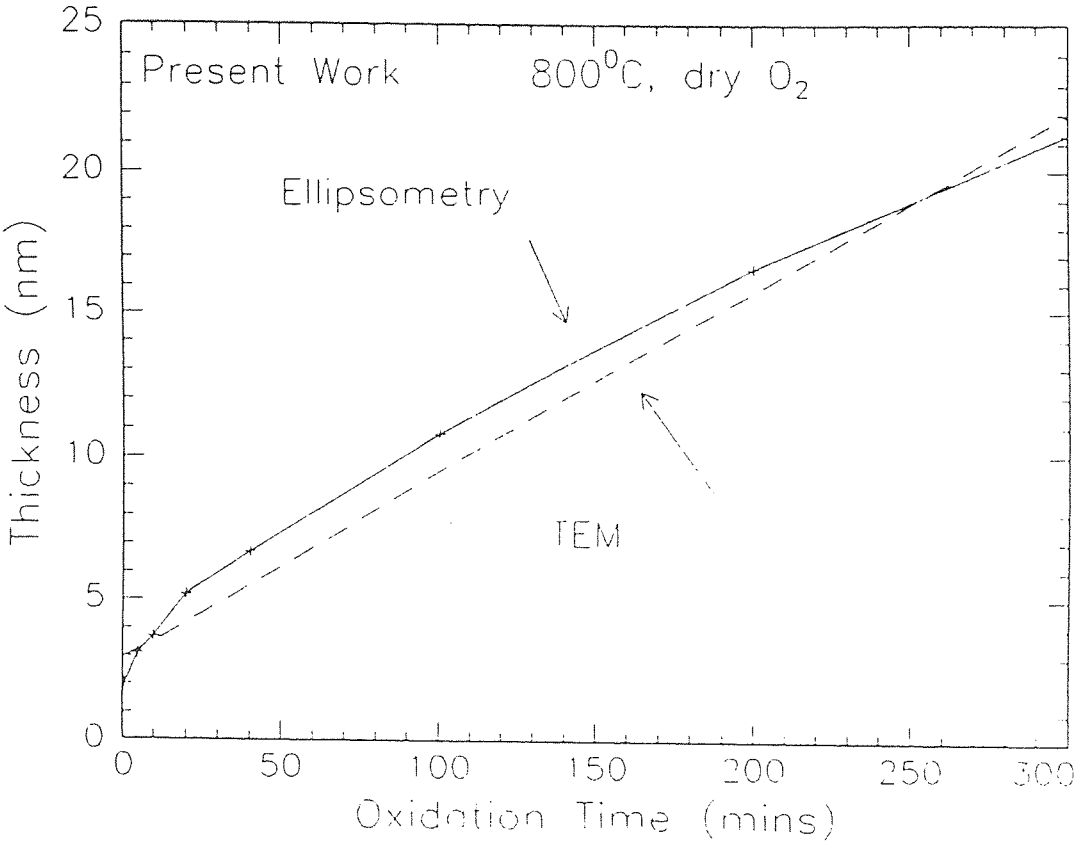


Figure 6.1: Plot of experimental data (Ellipsometry and TEM)

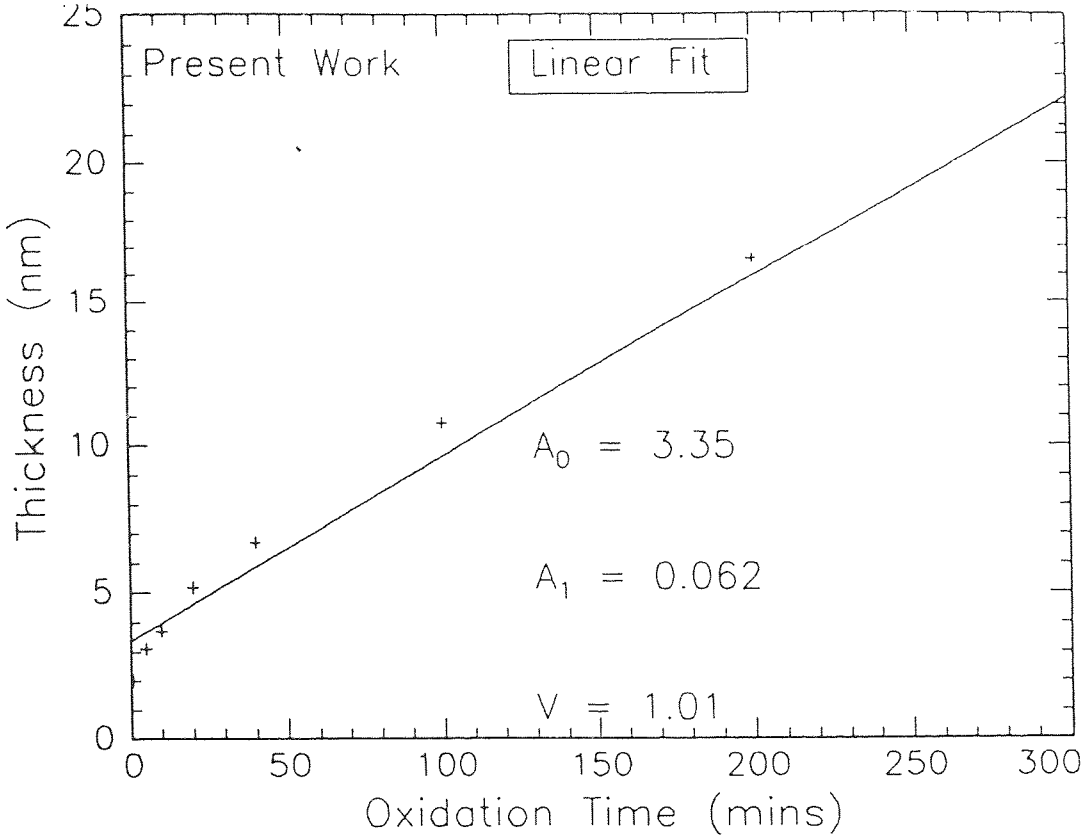


Figure 6.2: Linear fit to ellipsometric data

To compare possible formulations of the initial oxide growth law, it was assumed that all the oxides examined here were fabricated within the initial regime prior to Deal-Grove linear-parabolic oxidation and that approximation of the initial oxidation by a separate limiting expression is a reasonable simplification. The same thickness vs time data that is presented in Fig. 6.1 has been fitted to linear, parabolic, linear-parabolic, and variable power equations. Graphs illustrating the best fit of these equations to the data are shown in Figures 6.2 through 6.5. The coefficients for the fitted expressions are listed in Table 6.2.

The TEM data is fitted to linear and linear-parabolic expressions only as the plot clearly shows a linear trend. The fit to TEM data is shown in Fig 6.6 and Fig 6.7. The coefficients for the fitted expressions are listed in Table 6.3.

It is interesting to note that the linear-parabolic expression gives an excellent fit to the present data (Fig 6.4). The existence of the third adjustable parameter will always lead to a better fit for a linear-parabolic formulation, than is possible for either a linear or parabolic expression. The variable power law form which also pro-

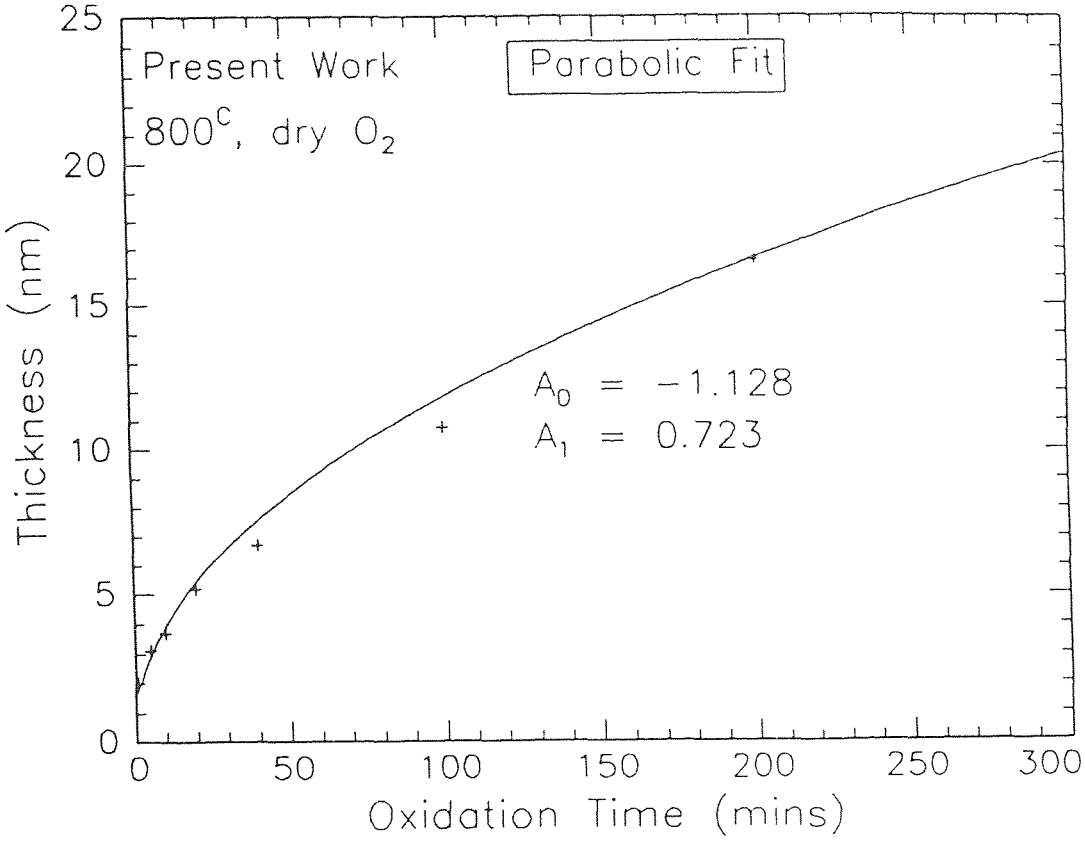


Figure 6.3: Parabolic fit to ellipsometric data

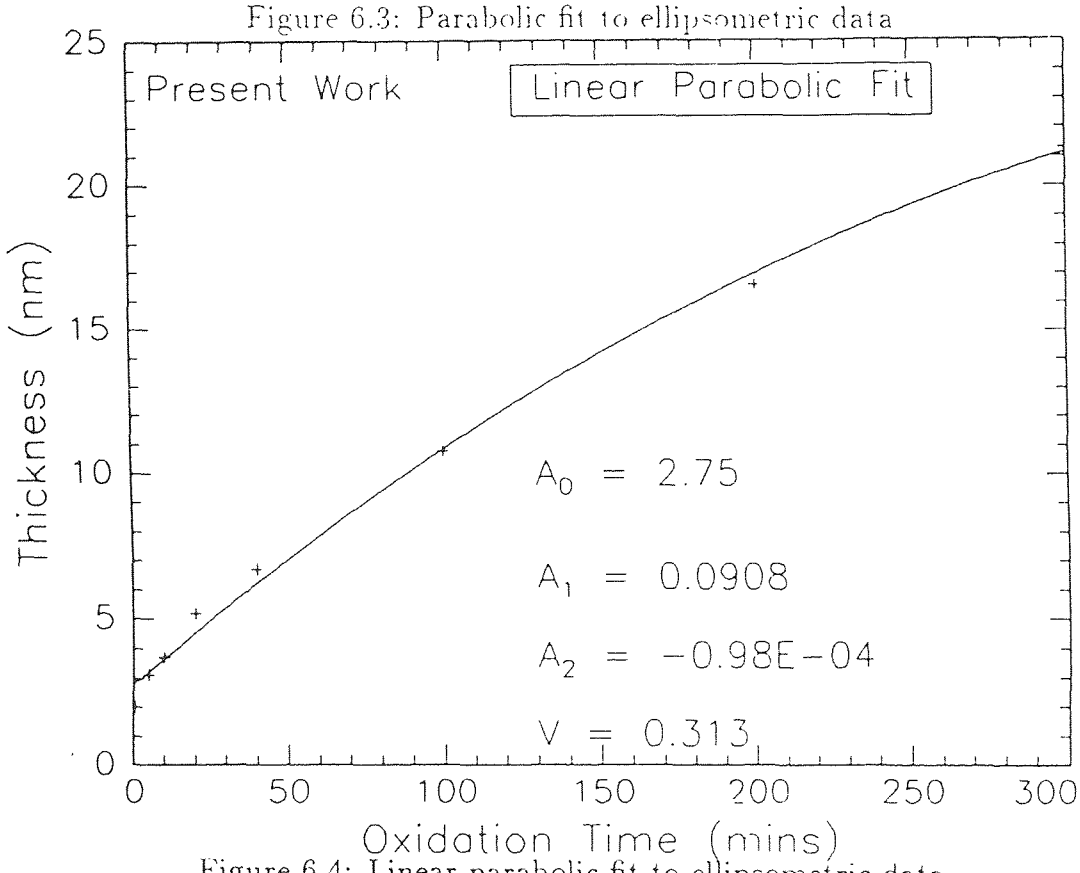


Figure 6.4: Linear-parabolic fit to ellipsometric data

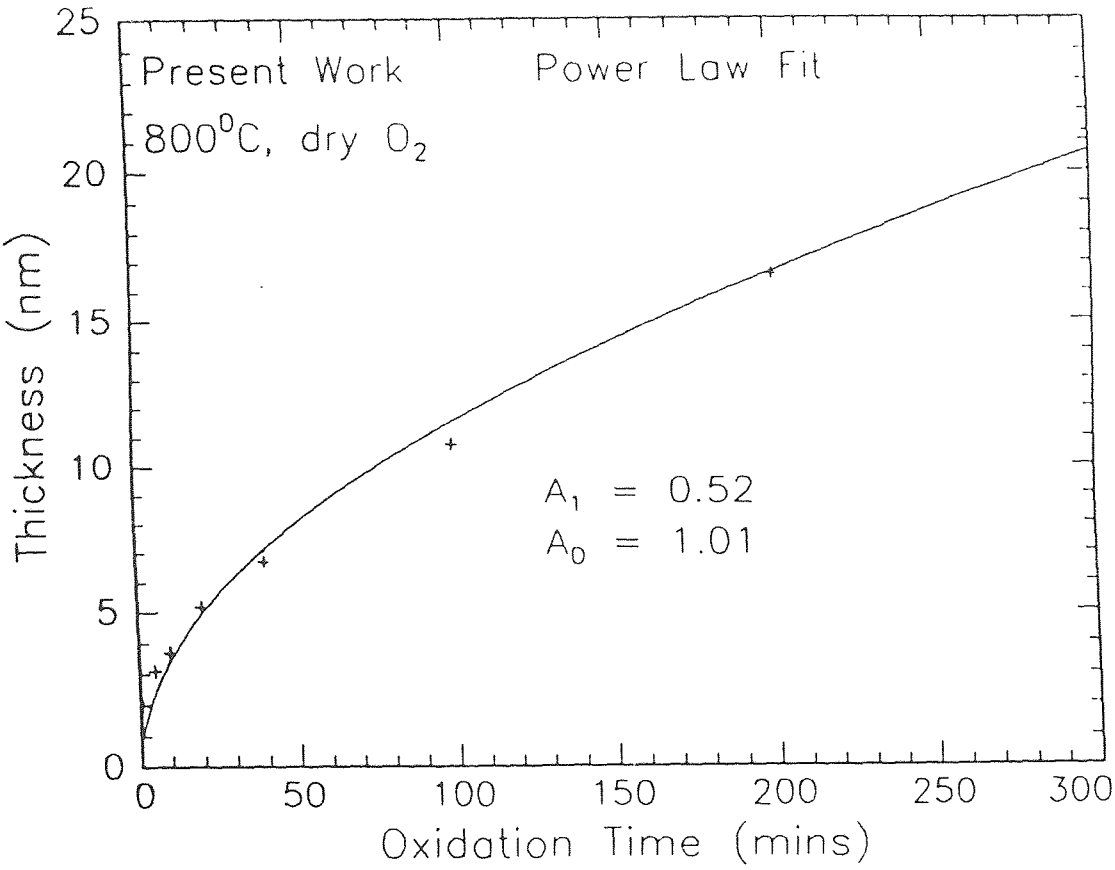


Figure 6.5: Variable power fit to ellipsometric data

$X = A_0 \cdot A_1 T$ LINEAR

$X = A_0 \cdot A_1 T^2$ PARABOLIC

$X = A_0 \cdot A_1 T \cdot A_2 T^2$ LINEAR-PARABOLIC

$X = A_0 T^{A_1}$ VARIABLE POWER

800 °C , DRY $O_2$

| | LINEAR | | PARABOLIC | | LINEAR - PARABOLIC | | | POWER | |
|---|---|---|---|---|---|---|---|---|---|
| | $A_0$ | $A_1$ | $A_0$ | $A_1$ | $A_0$ | $A_1$ | A | $A_0$ | $A_1$ |
| ELLIPSOMETRIC DATA | 3.35 | 0 062 | -1 128 | 0 06 | 2.75 | 0 098 | -0 9E-04 | 1 01 | 0 52 |

Table 6.2: Calculated Values of coefficients for linear, parabolic, linear- parabolic and variable power best fits to oxidation data from ellipsometry

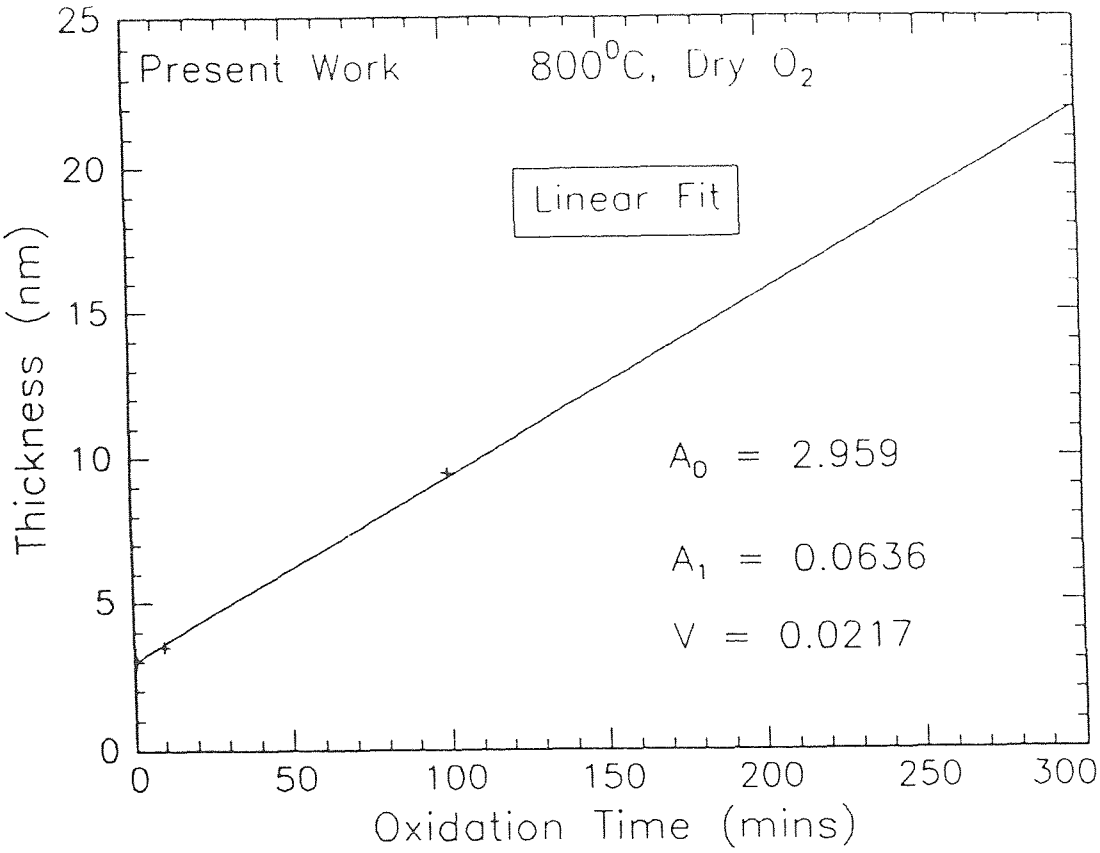


Figure 6.6: Linear fit to TEM data

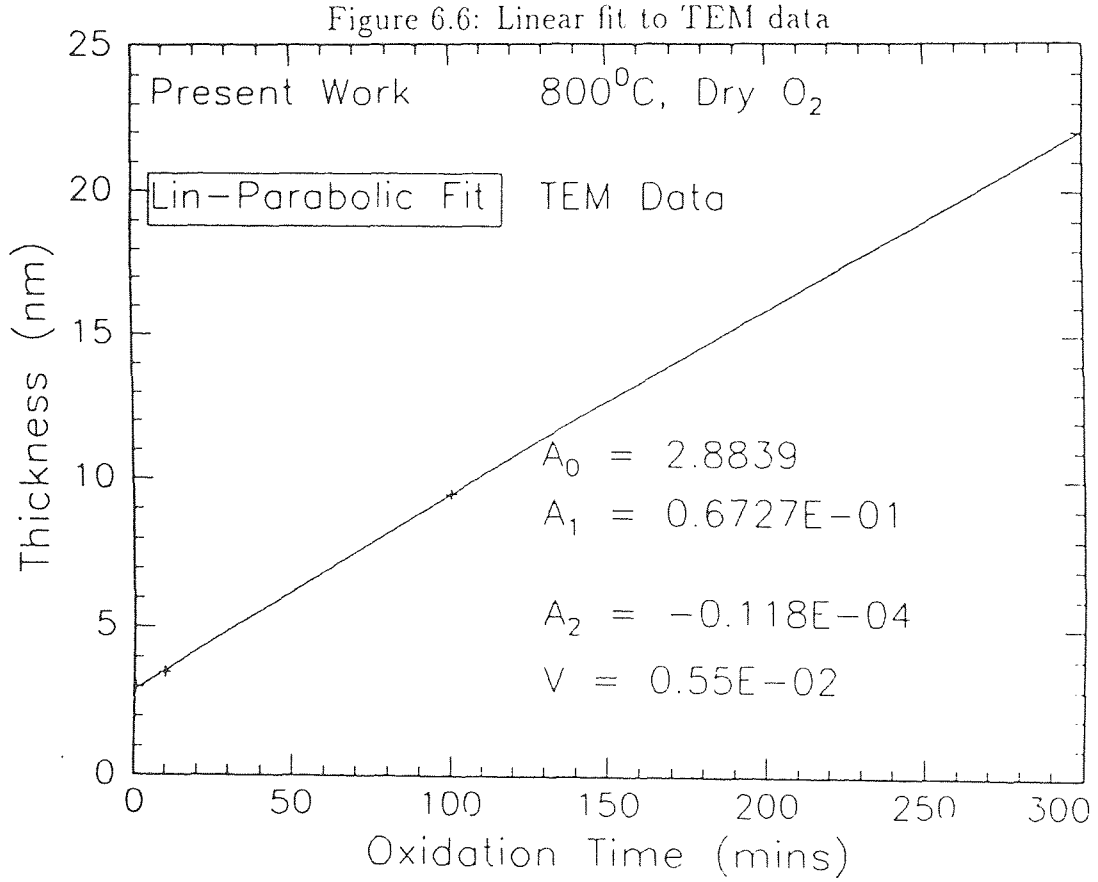


Figure 6.7: Linear-parabolic fit to TEM data

| 800 °C , DRY $O_2$, TEM DATA | | | | |
|---|---|---|---|---|
| LINEAR | | LINEAR-PARABOLIC | | |
| $A_0$ | $A_1$ | $A_0$ | $A_1$ | $A_2$ |
| 2.96 | 0.06 | 2.88 | 0.067 | -0.12E-04 |

Table 6.3: Calculated values of coefficients for linear and linear-parabolic best fits to TEM data

vided a reasonable representation of the oxide growth data, is physically unrealistic, since increasing growth rate is obtained. The excellence of the linear-parabolic fit for both ellipsometric and TEM data was further confirmed theoretically by simulating the expression by a computer program, with the coefficients obtained from the fit. The output (calculated value) gave a remarkable closeness to the experimental data. The results are shown in Table 6.4 and the program is shown in the appendix.

Several sets of data obtained from the work of other researchers were then analyzed by the present procedure, and in all cases the excellence of fit due to linear-parabolic model was observed. The fit to the published data is shown in figures 6.8 to 6.12. The constants obtained after the fit are described in Table 6.5. There is notable difference between the constants, but this phenomenon is well known to workers in this field. This indicates that oxidation data is process dependant, as for example the pre-oxidation surface cleaning procedure, partial pressures of the

| OXIDATION TIME (T) (MINS) | OXIDE THICKNESS | | | |
|---|---|---|---|---|
| | ELLIPSOMETRY | | HRTEM | |
| | EXPERIMENTAL (nm) | CALCULATED (nm) | EXPERIMENTAL (nm) | CALCULATED (nm) |
| 1 | 2.0 | 2.84 | 3.0 | 2.95 |
| 5 | 3.1 | 3.20 | | |
| 10 | 3.7 | 3.65 | 3.5 | 3.55 |
| 20 | 5.2 | 4.53 | | |
| 40 | 6.7 | 6.23 | | |
| 100 | 10.8 | 10.85 | 9.5 | 9.46 |
| 200 | 16.6 | 16.99 | | |
| 300 | 21.3 | 21.17 | 22.0 | 21.90 |

Table 6.4: Experimental and Calculated values to demonstrate the excellence of linear-parabolic fit to the experimental data

chemical species, temperature and its uniformity, orientation and resistivity of the wafers etc.

The linear-parabolic fits give an extrapolated "initial" oxide thickness of 2.75 nm prior to oxidation. This initial thickness is similar to the values of 2.7 nm and 2.5 - 3.0 nm derived by other workers[34,35], although with different techniques. This is due to the native oxide thickness and the oxide formed during the insertion of wafers into the furnace and ramp up of to temperature.

The most striking facet of these work is that although the linear-parabolic expression gives an excellent fit to the ellipsometric data, it is less accurate when applied to the HRTEM data, which clearly shows a linear trend. The implication is that although the optical thickness of the oxide may develop according to a linear-parabolic law, the structural thickness increases linearly with time in the initial region. However, there are uncertainties in both techniques : (a) In single-wavelength or spectroscopic ellipsometry, a prior knowledge of the refractive index

| LINEAR-PARABOLIC FIT | | | |
|---|---|---|---|
| Reference | $A_0$ | $A_1$ | $A_2$ |
| Present Work | 2.75 | 0.0908 | -0.98E-04 |
| Carim et al. | 2.995 | 0.0089 | -0.16E-05 |
| Massoud et al. | 1.984 | 0.065 | -0.41E-04 |
| A. Reisman et al. | 7.3 | 0.487 | -0.31E-04 |
| L. N. Lie et al. | 15.3 | 0.26 | -0.58E-04 |
| Deal & Grove | 24.21 | 0.039 | -0.20E-05 |

Table 6.5: Coefficients obtained from linear-parabolic fitting of published experimental data

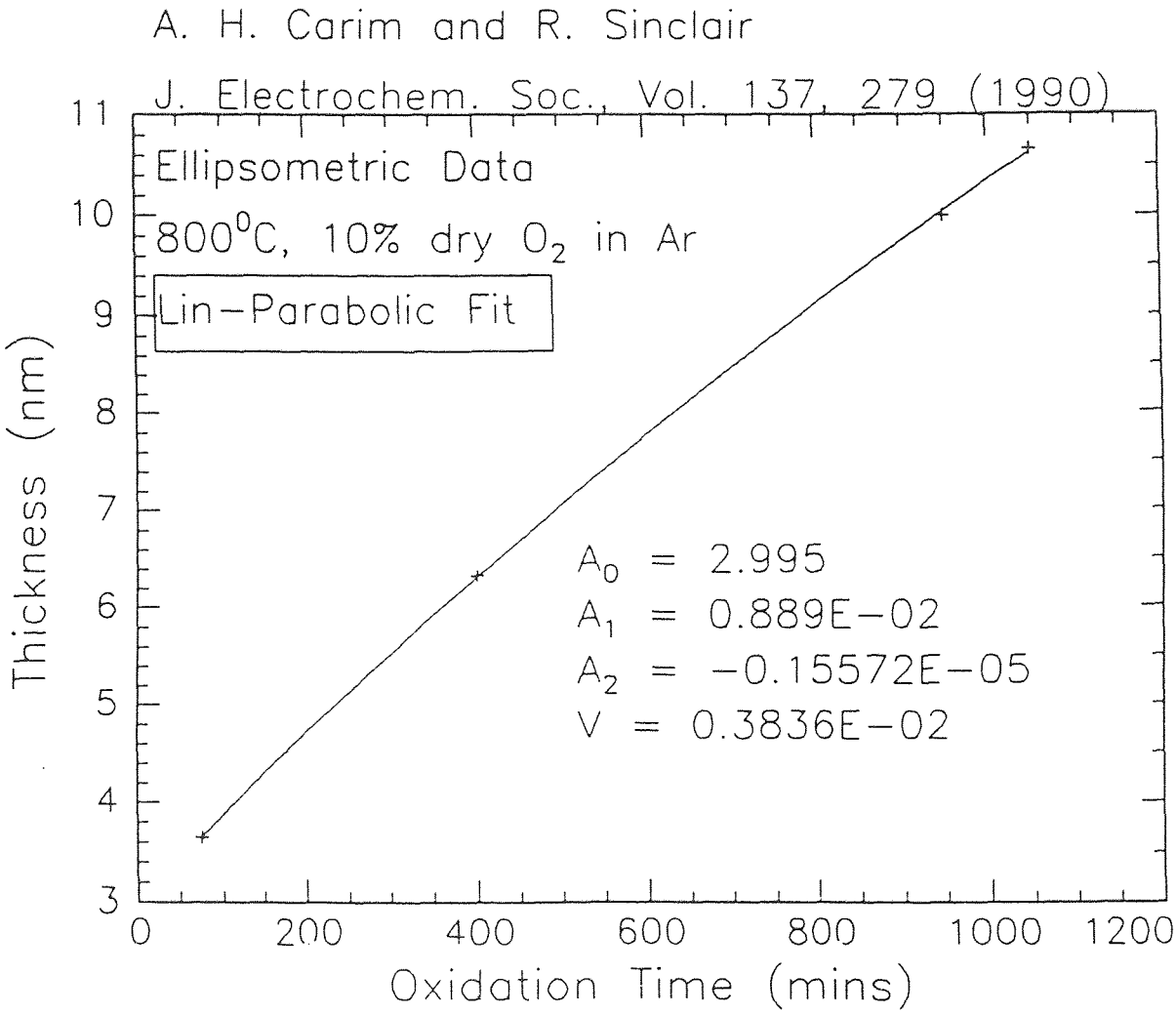


Figure 6.8: Linear-Parabolic fit to published data by Carim[14]

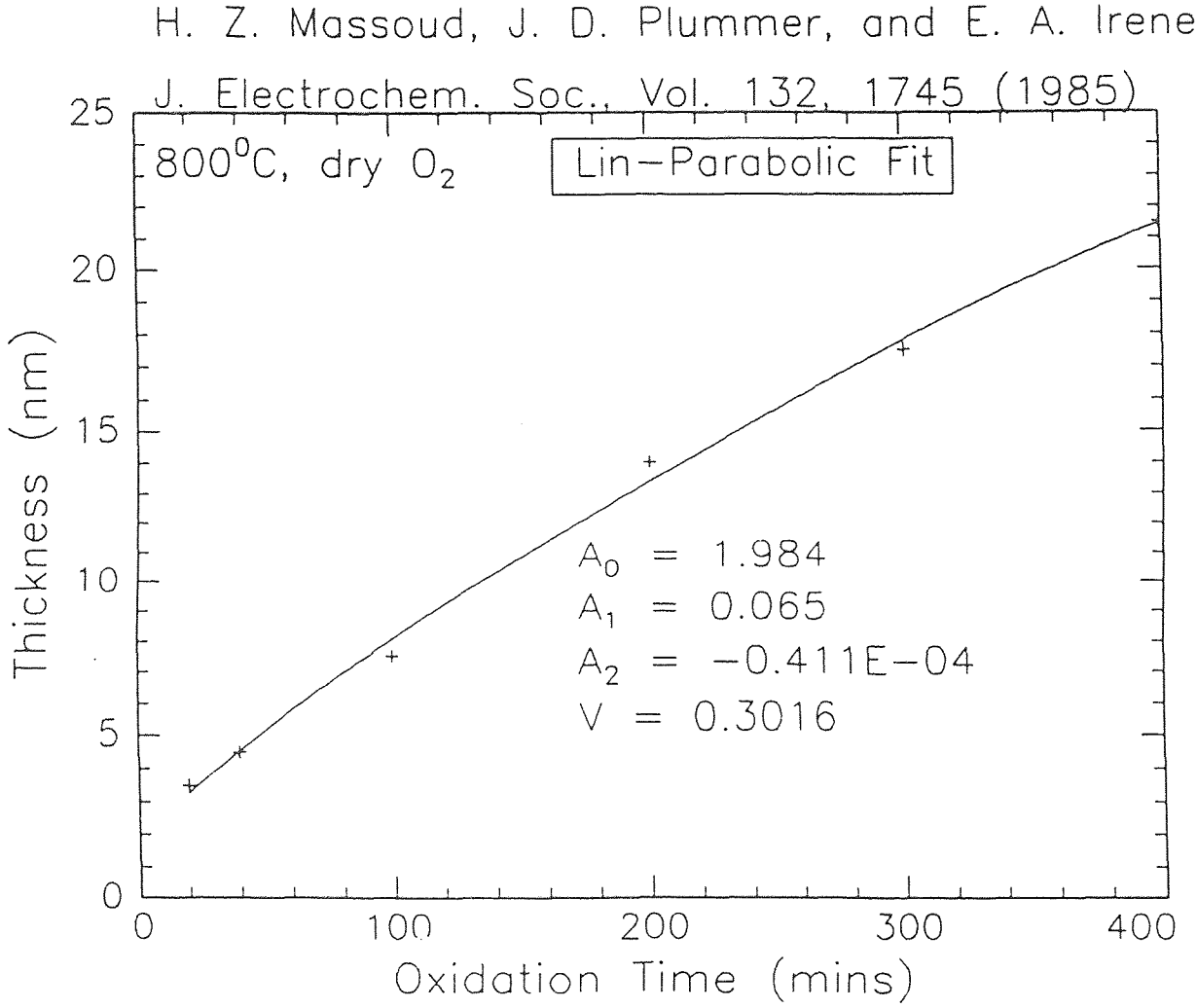


Figure 6.9: Linear-Parabolic fit to published data by Massoud et al.[30]

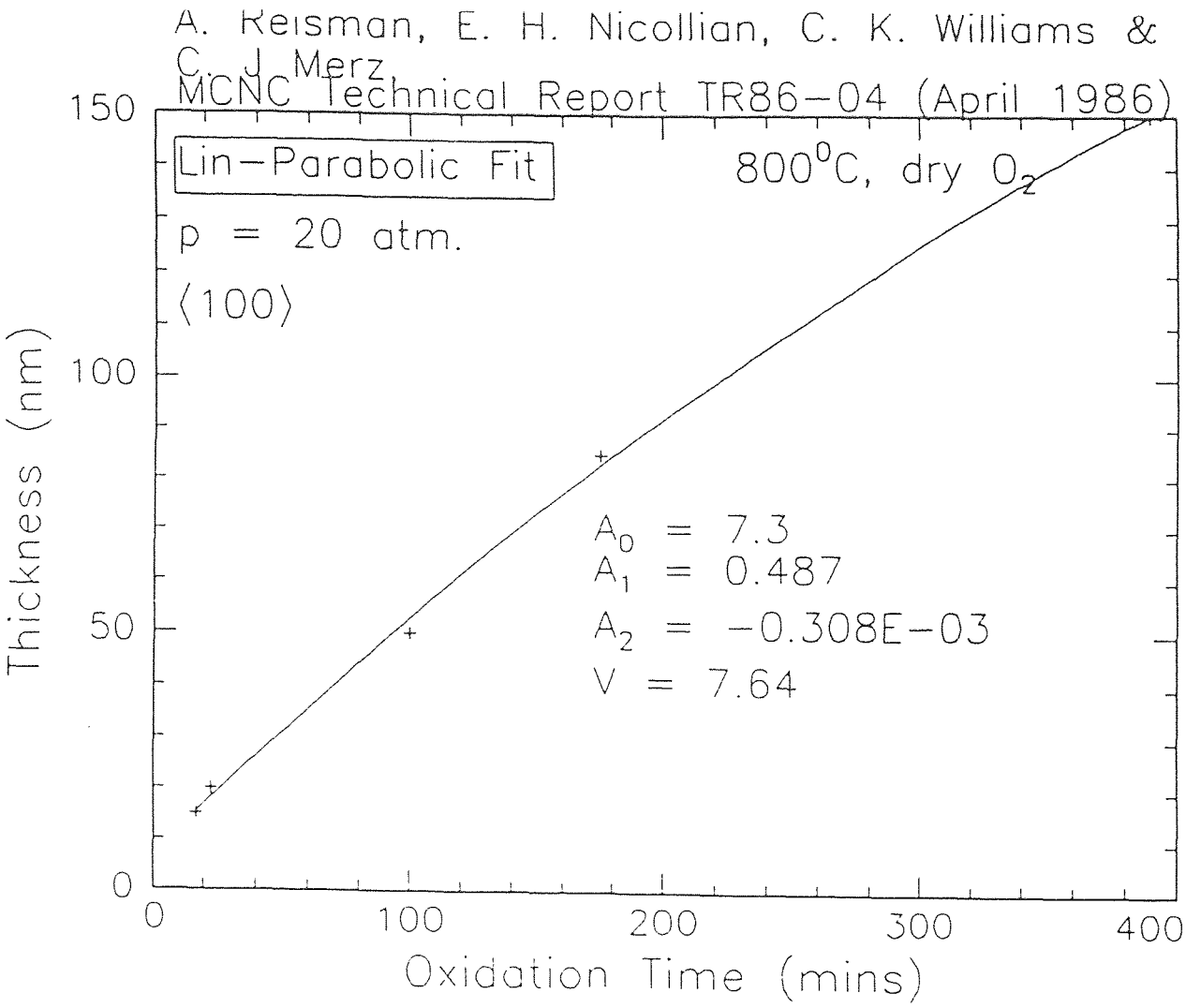


Figure 6.10: Linear-Parabolic fit to published data by A. Reisman et al.[29]

and extinction coefficient of $SiO_2$ is required in order to evaluate thickness. These values are dependent on the wavelength of the incident radiation and the oxide thickness, especially, for very thin films that are a few monolayers thick. (b) In HRTEM, the oxide thickness measurements are complicated by the very nature of the interface. Further, as much as the method is destructive, one needs to perform these measurements on many samples from each wafer in order to map thickness as function of position on the wafer.

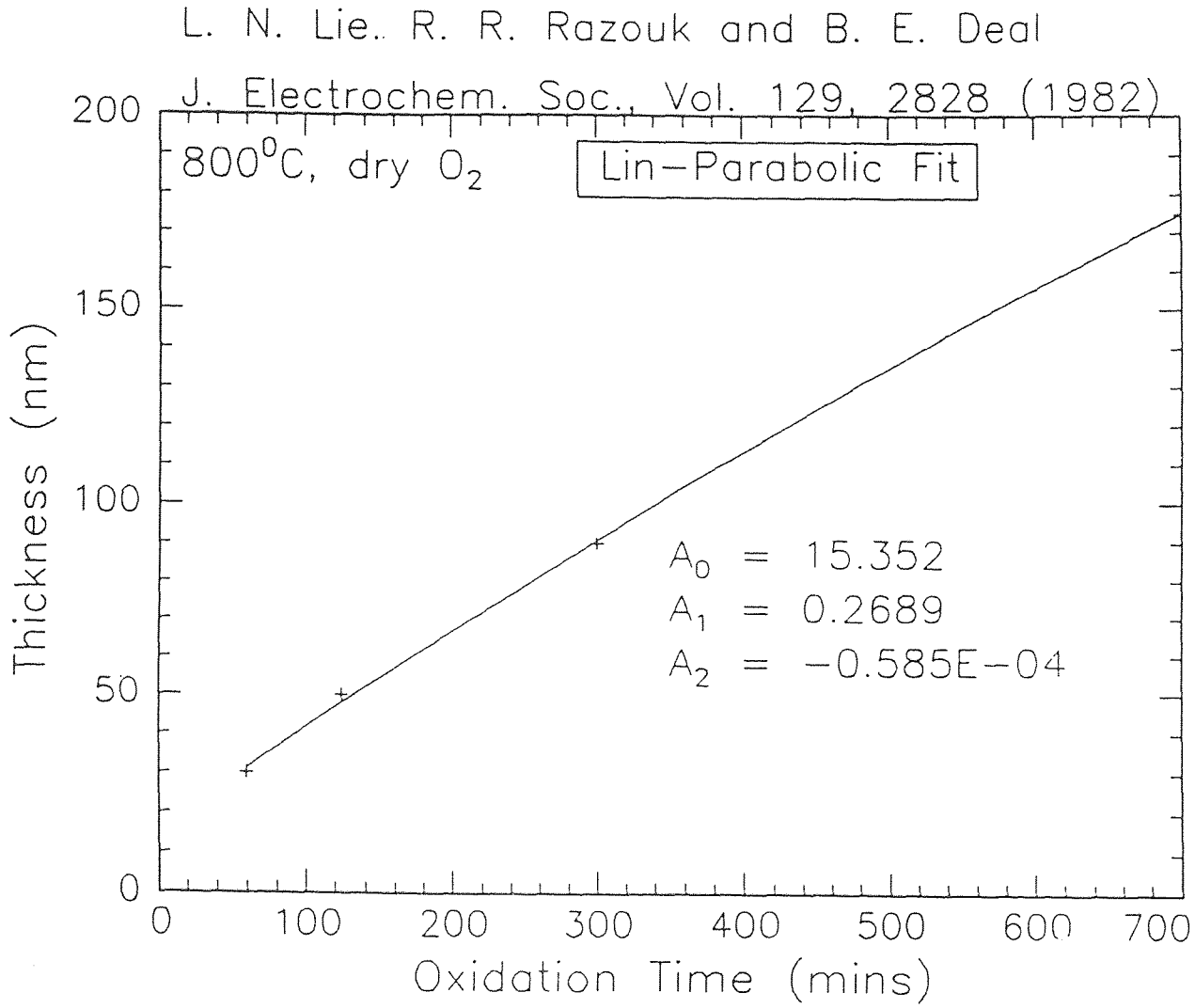


Figure 6.11: Linear-Parabolic fit to published data by L.N. Lie et al.[22]

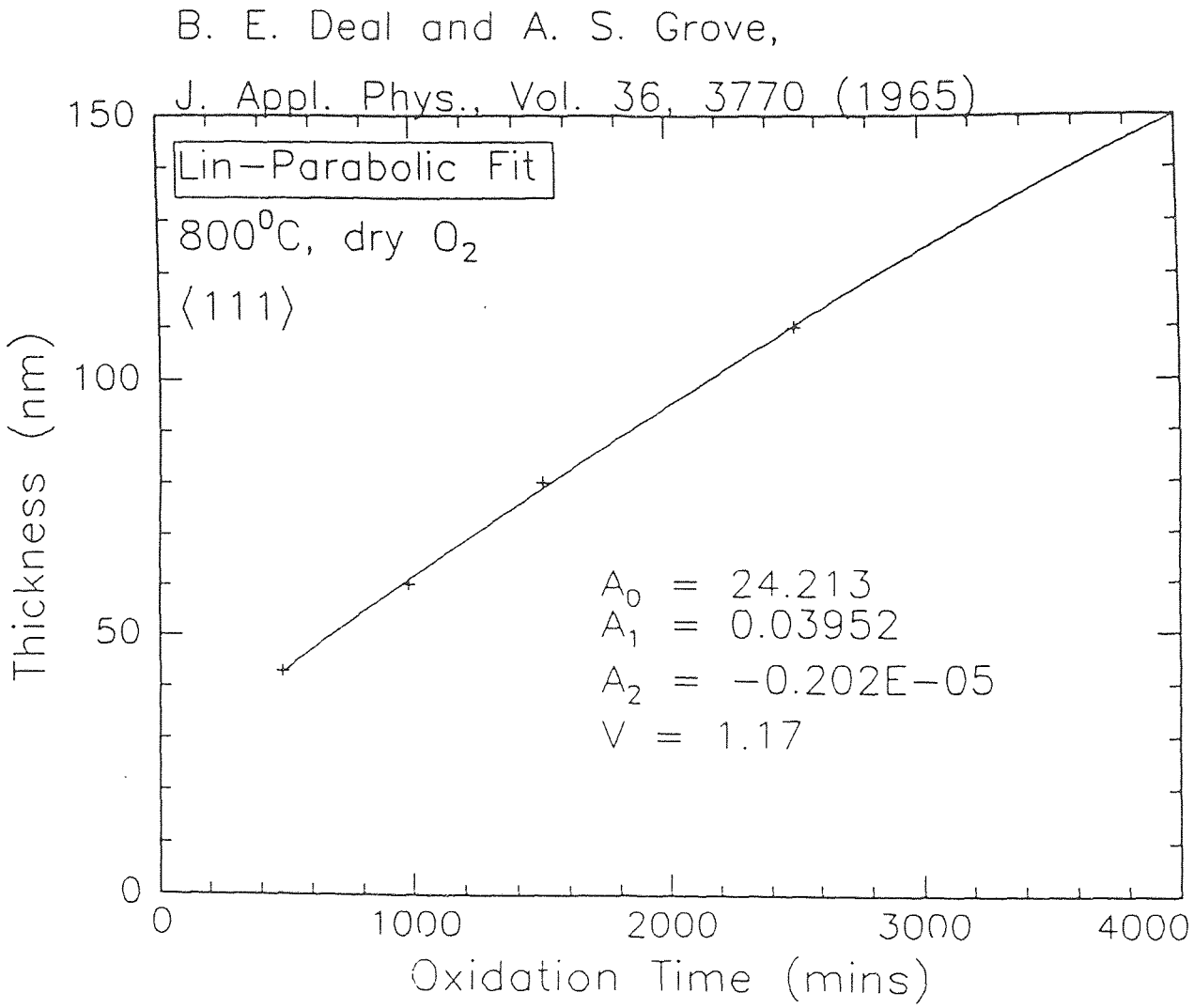


Figure 6.12: Linear-Parabolic fit to published data by Deal and Grove[6]

# Chapter 7

# Conclusion

An analysis of the various models, proposed in the literature, for explaining the oxidation kinetics of silicon in the thin oxide regime, has been presented in this study. This analysis considers recently reported measurements of thicknesses of $SiO_2$ films grown thermally on Si at $800^oC$ for time durations of 1-300 minutes in dry $O_2$, using the techniques of HRTEM and ellipsometry. The ellipsometric data obtained from this work as well as from other researchers, showed an excellence of fit to the linear-parabolic formulation of Deal and Grove. However the HRTEM data are somewhat different, and showed an initial linear regime.

Direct observation of thin oxide films in cross-section by high resolution electron microscopy demonstrate that the structural thickness is somewhat less than that indicated by ellipsometric measurements. The discrepancy is due to the fact that ellipsometry measures an effective "optical thickness" and makes a number of

assumptions when identifying that value with the structural thickness of the oxide layer.

It may also be noted that several assumptions must be made in order to obtain thickness information for thin oxides by ellipsometry. The optical constants must be obtained from thicker oxide films, so it must have been assumed that they are independent of film thickness during oxide growth. However some recent studies have shown, this is not the case.

The literature in this area is voluminous and therefore this survey, should not be construed as exhaustive or complete. It now rest on readers to undergo further research, based on the current work and come up with solutions to the unanswered queries.

# Bibliography


[1] N.M. Ravindra et al., Proc. of the SPIE Conference on Semiconductors '88, Vol. 945, 84(1988)

[2] G.R. Wolstenholme et al., J. Appl. Phys. Vol. 61, 225(1987).

[3] H.C. deGraff and J.G. deGroot, IEEE Trans. Electron Devices ED-26, 1771(1979).

[4] G.L. Patton et al., IEEE Trans. Electron Devices ED-33, 1754(1986).

[5] H.H. Busta and C.H. Tang, J. Electrochem. Soc. Vol. 133, 1195(1986).

[6] B.E. Deal and A.S. Grove, J. Appl. Phys. Vol. 36, 3770(1965).

[7] W.A. Tiller, J. Electrochem. Soc. Vol. 127, 625(1980).

[8] A. Fargeix et al., J. Appl. Phys. Vol. 54, 2878(1983).

[9] S.A. Schafer and S.A. Lyon, Appl. Phys. Lett. Vol. 47, 154(1985).

[10] S.M. Sze, Semiconductor Devices, Physics and Technology, (1985).

[11] E.H. Nicollian and J.R. Brews, MOS Physics and Technology, Wiley, New York, 1982.

[12] N.M. Ravindra et al., Proc. Mat. Res. Soc., Vol. 105, 169(1988).

[13] S.M. Sze(ed.), VLSI Technology, p.98, McGraw-Hill, NY, 1983.

[14] A. Carim, Ph.D. dissertation, Stanford University, Stanford, CA(1989).

[15] J.D. Plummer in Semiconductor Silicon, pp 445-54(1981).

[16] E.A. Irene, J. Electrochem. Soc., Vol. 125, 1708(1978).

[17] A.C. Adams et al., J. Electrochem. Soc., Vol. 127, 1787(1980).

[18] S. Wolf and R.N. Tauber, Silicon Processing in VLSI Era, Vol. 1, 1990.

[19] Y.C. Cheng and B.Y. Liu, J. Electrochem. Soc., Vol. 131, 354(1984).

[20] F.N. Schwettmann et al., Proc. of the 153rd Electrochem. Soc. Meet., The Electrochem. Soc., Princeton, NJ, 688(1978).

[21] R.A. Levy(ed.), Microelectronic Materials and Processes, 79(1989).

[22] L.N. Lie et al., J. Electrochem. Soc., Vol. 132, 2685(1985).

[23] N.M. Ravindra et al., Materials Letters, Vol. 4, 337(1986).

[24] E.P. EerNisse, Appl. Phys. Lett., Vol. 35, 8(1979).

[25] Y.J. Van der Meulen, J. Electrochem. Soc., Vol. 119, 530(1972).

[26] E.A. Irene, J. Electrochem. Soc., Vol. 125, 1708(1978).

[27] V. Murali and S.P. Murarka, J. Appl. Phys., Vol. 60, 2106(1986).

[28] M.A. Hooper et al., J. Electrochem. Soc., Vol. 122, 1216(1975).

[29] A. Reisman et al.,MCNC Technical Report, TR86-04, April(1986).

[30] H.Z. Massoud et al., J. Electrochem. Soc., Vol. 132, 2693(1985).

[31] P.J. McMarr et al., J. Appl. Phys., Vol. 59, 694(1986).

[32] N.M. Ravindra et al., J. Mat. Res., Vol. 2, 216(1987).

[33] GENPLOT, Computer Graphics Services(1986).

[34] K.K. Ng et al., App. Phys. Let., Vol. 44, 626(1984).

[35] J. Wong et al., App. Phys. Let., Vol. 48, 65(1986).

# Appendix

# C PROGRAM TO SIMULATE THE LINEAR PARABOLIC MODEL

```
\*************************************************************************\
\* PROGRAM WRITTEN BY TIRTHANKAR DUTTA AS A PART OF THE MASTERS THESIS *\
\*************************************************************************\
\* This program simulates the Linear Parabolic function with the calculated *\
\* constants, and the time intervals at which the actual experimental  *\
\* observations were done for the ellipsometric data.                  *\
\*************************************************************************\
#include <stdio.h>
#include <math.h>
main()

{
\*************************************************************************\
\* The constants obtained from the linear-parabolic fit are defined here *\
\*************************************************************************\
float A0 =  2.75;
float A1 =  0.0908 ;
float A2 = -0.98E-04 ;
\*************************************************************************\
\* The time intervals at which the observations were made are defined here *\
\*************************************************************************\
static int T[8] = { 1, 5, 10, 20, 40, 100, 200, 300 };
int   i ;
float x ;

printf("\n");
printf("\*************************************************************\n");
printf("                P R O G R A M          O U T P U T             \n");
printf("\*************************************************************\n");
printf("\n");
printf("\n");
printf("            L I N E A R      P A R A B O L I C          F I T \n");
printf("            ---------------------------------------------\n");
printf("\n");
printf("\n");
printf("               ( E L L I P S O M E T R I C     D A T A ) \n");
printf("\n");
printf("\n");
printf("      (Calculated values with coefficients obtained from fit ) \n") ;
printf("\n");
printf("\n");
printf("                          T(hrs)          x(nm)\n");
printf("                          ------------------\n");
printf("\n");
printf("\n");
for  ( i = 0 ; i <= 7 ; ++i)
{
x = (   A0 + (A1*T[i]) + (A2*T[i]*T[i]) ) ;
printf("                          %3d             %4.2f \n", T[i], x ) ;
printf("\n") ;
printf("\n");
printf("\*************************************************************\n");
}
}
```

```
\*************************************************************************\
\* PROGRAM WRITTEN BY TIRTHANKAR DUTTA AS A PART OF THE MASTERS THESIS *\
\*************************************************************************\

\* This program simulates the Linear Parabolic function with the calculated *\
\* constants, and the time intervals at which the actual experimental  *\
\* observations were done for the TEM data.                            *\
\*************************************************************************\

#include <stdio.h>
#include <math.h>
main()

{

\*************************************************************************\
\* The constants obtained from the linear-parabolic fit are defined here *\
\*************************************************************************\

float A0 =  2.88;
float A1 =  0.067 ;
float A2 = -0.12E-04 ;

\*************************************************************************\
\* The time intervals at which the observations were made are defined here *\
\*************************************************************************\

static int T[4] = { 1, 10, 100, 300 };
int   i ;
float x ;
printf(" \n");
printf(" ************************************************************\n");
printf("                P R O G R A M          O U T P U T \n");
printf(" ************************************************************\n");
printf(" \n");
printf(" \n");
printf("            L I N E A R      P A R A B O L I C       F I T   \n");
printf("            ---------------------------------------------   \n");
printf("\n");
printf("\n");
printf("                      ( H R T E M     D A T A )                \n");
printf("\n");
printf("\n");
printf("x = A0 + A1*T + A2*T*T \n");
printf("\n");
printf("\n");
printf("    ( Calculated values with coefficients obtained from the fit )\n");
printf("\n");
printf("\n");
printf("                          T(hrs)          x(nm)\n");
printf("                          ---------------------\n");
printf("\n");
printf("\n");
for  ( i = 0 ; i <= 3 ; ++i)
{
x = (   A0 + (A1*T[i]) + (A2*T[i]*T[i]) ) ;
printf("                          %3d             %4.2f \n", T[i], x ) ;
printf("\n") ;
printf("\n");
printf(" ************************************************************\n");
}
}
```